MARMARA UNIVERSITY
INSTITUTE FOR GRADUATE STUDIES
IN PURE AND APPLIED SCIENCES

CBD LOADED *HALOMONAS* LEVAN HYDROGELS FOR PREVENTION OF MEDICATION RELATED OSTEONECROSIS OF THE JAW (MRONJ)

ECE ÖZYAĞCI

MASTER THESIS
Department of Bioengineering

Thesis Supervisor
Prof. Ebru TOKSOY ÖNER

ISTANBUL, 2024

MARMARA UNIVERSITY
INSTITUTE FOR GRADUATE STUDIES
IN PURE AND APPLIED SCIENCES

CBD LOADED *HALOMONAS* LEVAN HYDROGELS FOR PREVENTION OF MEDICATION RELATED OSTEONECROSIS OF THE JAW (MRONJ)

ECE ÖZYAĞCI
(524221019)

MASTER THESIS
Department of Bioengineering

Thesis Supervisor
Prof. Ebru TOKSOY ÖNER

ISTANBUL, 2024

ACKNOWLEDGEMENTS

I have experienced and learned a lot of things during my master's thesis adventure. I would like to express my thanks to the valuable people, and institutes, who supported me and my thesis in this important and challenging journey. Firstly, I would like to express my gratitude and respect to my meritorious thesis supervisor Prof. Ebru Toksoy Öner. I feel thankful for her wonderful guidance, kindness, and the opportunities that she provided. This thesis was a part of the project titled "INJECT-BIO Bioactive injectable hydrogels for soft tissue regeneration after reconstructive maxillofacial surgeries" and was supported by The Scientific and Technological Research Council of Turkey (TUBITAK) with the project number 119N756. I would like to thank to my friends (from Industrial Biotechnology and Systems Biology (IBSB) research group), Selay Tornacı and Rüya Giray, for sharing their experiences and advice tirelessly; Hümeyra Aydın, Berkay Göktuğ Avcı, and Aybüke Tekin for their support and advices. Their friendship made my master's thesis period more meaningful. Finally, thanks to my family, Aysel Özyağcı, Ümit Özyağcı, and Doğa Özyağcı who brought me to today with their endless support and love.

Ece Özyağcı

TABLE OF CONTENTS

ÖZET

İLACA BAĞLI OLARAK ÇENE KEMİKLERİNDE GÖRÜLEN OSTEONEKROZ (MRONJ) HASTALIĞININ CBD YÜKLÜ *HALOMONAS* LEVAN HİDROJELLER İLE ÖNLENMESİ

İlaca bağlı olarak çene kemiklerinde görülen osteonekrosis (MRONJ), hastaların hayat kalitesini ağrı, diş gevşemesi, açık yara, ve kemik nekrozu ile düşüren bir hastalıktır. Geçmişte bisfosfonat ve denosumab kullanmış olan insanlar MRONJ riski taşımaktadır. Özen gösterilen ağız hijyeni hastalığı önlemeye yardımcı olmaktadır. Yine de, polimer hidrojel sistemleri bölgeye kontrollü ilaç salınımı sağlayarak hastalığın önlenmesi veya tedavisine yönelik çalışmalara konu olmaktadır. Hücre dışı matriksi taklit eden yapısı olan ve yüksek miktarda su tutabilen hidrojeller, ilaç taşıma sistemi olarak ve hücre adezyonu ve proliferasyonu için uygun bir ortam sağlayarak doku mühendisliğinde kullanılmaktadır.

Levan, β-2,6 bağlı fruktozil kısımları bulunan, çeşitli mikroorganizmalar ve bitkiler tarafından üretilen bir fruktan ekzopolisakkaritidir. Biyouyumluluk özelliği ile eczacılık, kozmetik, ve gıda alanlarında kullanılmaktadır. Kannabidiol (CBD), psikoaktif olmayan, antienflamatuar, ve ağrı kesici özellikleri bulunan, *Cannabis sativa* bitkisinin içerdiği hidrofobik bir bileşiktir. Bu tez çalışmasında, levan bazlı, 1,4-butandiol diglisidil eter BDDE çapraz bağlanmış hidrojeller geliştirerek mekanik özelliklerini (şişme, jel fraksiyonu, stabilite) incelemek ve CBD ile HOB hücreleri üzerindeki sitotoksisitesini incelemek hedeflenmiştir. Bu doğrultuda, operasyon bölgesinde olası ağrıyı keserek ve hücre proliferasyonunu destekleyerek MRONJ hastalığını engellemek üzere levan ve CBD içeren hidrojeller üretilmiştir.

Düzensiz şekildeki boşlukların doldurulmasının kolaylaştırılması için parçalanan hidrojellerin CBD salınım profili, parçacık boyutu, ve polidispersite indeksi incelenmiştir. Öğütülmüş 1:35 levan hidrojeller yüksek jel fraksiyonları ile biyouyumlu ve şekillendirilmesi kolay olarak değerlendirilmiştir. Hidrojelden gerçekleşen CBD salınımı sonuçları HOB hücrelerine toksik olmayan konsantrasyonda seyretmiştir.

ABSTRACT

CBD LOADED *HALOMONAS* LEVAN HYDROGELS FOR PREVENTION OF MEDICATION RELATED OSTEONECROSIS OF THE JAW (MRONJ)

Medicine related osteonecrosis of the jaw (MRONJ) is a disease that lowers the life quality of the patients with the pain, teeth loosening, open wound, and necrosis of the bone. People who have used bisphosphonates denosumab in their past have the risk of MRONJ. Careful oral hygiene helps to prevent the disease, however, polymer hydrogel systems are widely studied to prevent or cure the disease by providing a controlled drug release. Biomaterials like hydrogels, which mimic the extracellular matrix (ECM) and can keep a high amount of water, are used as drug delivery systems and in tissue engineering by providing a proper environment for cell adhesion and proliferation.

Levan is a fructan exopolysaccharide with β-2,6 linked fructosyl residues produced by various microorganisms and plants. It is biocompatible and used in pharmaceutics, cosmetics, and food. Cannabidiol (CBD) is a hydrophobic compound of the plant *Cannabis sativa* and has non-psychoactive, anti-inflammatory, and pain relief properties.

The aim of this thesis was to develop a levan based 1,4-butanediol diglycidyl ether (BDDE) crosslinked hydrogel, examining its mechanical properties (swelling, gel fraction, stability) and cytotoxicity with CBD on HOB cells. For this, the hydrogels that include these two ingredients, were produced to prevent MRONJ by supporting the cell proliferation and relieving the pain in the operation area.CBD release profile, particle size, and polydispersity index of shredded hydrogels were also examined to ease the application to the cavities that have irregular shape. 1:35 ground hydrogels with high gel fraction were found to be biocompatible and easy to shape. CBD release was observed between the non-toxic range of concentrations to HOB.

SYMBOLS

% : Percentage

µl : Microliter

µm : Micrometer

°C : Celsius degree

CO_2 : Carbon dioxide

CV : Column volume

d.nm : Nanometer (diameter)

g/g : Gram per gram

g : Gram

M : Molar

mg/ml : Milligram per milliliter

ml : Milliliter

nm : Nanometer

rcf : Relative centrifugal force

rpm : Revolutions per minute

w/v : Weight per volume

M_n : Number average molecular weight

M_w : Weight average molecular weight

Da : Daltons

ABBREVIATIONS

3D : Three Dimensional
BDDE : 1,4-butanediol diglycidyl ether
CB1 : Cannabinoid receptor type 1
CB2 : Cannabinoid receptor type 2
CBD : Cannabidiol
CCK-8 : Cell Counting Kit-8
DEAE : Diethylaminoethyl
DLS : Dynamic Light Scattering
ECM : Extracellular Matrix
EDTA : Ethylenediaminetetraacetic acid
EtOH : Ethanol
FTIR : Fourier Transform Infrared Spectroscopy
GPC : Gel Permeation Chromatography
HBO : Hyperbaric Oxygen Therapy
HOB : Human Osteoblast Cell line
IMAC : Immobilized Metal Affinity Chromatography
IPTG : Isopropyl β-D-1-thiogalactopyranoside
LB : Luria Broth
MRONJ : Medicine Related Osteonecrosis of the Jaw
OD : Optical Density
PBS : Phosphate Buffered Saline
PdI : Polydispersity Index
PEG : Polyethylene glycol
PLGA : Poly (Lactide-*co*-Glycolide)
PNIPAM : Poly(N-isopropyl acrylamide)
PVA : Poly (vinyl) alcohol
UV : Ultraviolet

LIST OF FIGURES

LIST OF TABLES

1. INTRODUCTION

1.1. Medicine Related Osteonecrosis of Jaw (MRONJ)

Bisphosphonates and denosumab are used in the treatment of calcium metabolism and tooth diseases. Bisphosphonates restrict calcium phosphate crystal formation (Fleisch et al., 2002) and can be used in cancer cell inhibition, hypercalcemia, and fibrous dysplasia (Kuźnik et al., 2020). Both bisphosphonates and denosumab reduce bone resorption (Fleisch et al., 2002; AlRowis et al., 2022). MRONJ is a jawbone death disease that can occur when patients have used denosumab and bisphosphonates related medicines and it can be triggered with teeth extraction (AlRowis et al., 2022; Hasegawa et al., 2017). It affects the life quality of the patient by causing pain in every stage of the disease and an open wound comes with the necrosis of bone in the later stages. Mandible bone pain, sinus pain, and teeth loosening can be seen in stage 0 with no evidence of bone necrosis (AlRowis et al., 2022). At stage 1, necrotic bone is observed without infection. When the infection starts along with the bone necrosis, the disease is called stage 2. In addition to the symptoms seen at stage 2, oroantral fistula, extraoral fistula, and necrotic bone explosion in the maxillary sinus are seen in stage 3 (On et al., 2021).

Different stages of MRONJ require different treatments. Patients should be aware of the risk of MRONJ by checking their medical history; thus, precautions can be taken beforehand for the MRONJ treatment. Antibiotics, hyperbaric oxygen therapy (HBO), parathyroid hormone, and bone morphogenic protein treatment are used as non-operational treatments at the lower stages of the disease (Jiang et al., 2024). Necrotic bone resection is applied as operational treatment for the following stages. Wilde et al. (2011) cover the operation area with a bilayer wound closure after bone resection.

Hydrogels have a high capacity to hold water in their extracellular matrix (ECM) mimicking structure. These scaffolds are widely used in tissue engineering for wound healing and also to prevent and treat the MRONJ or other mandibular defects by releasing active reagents (Guo et al., 2023; Brierly et al., 2019). Both injectable and non-injectable hydrogels are studied to fill the extraction socket (Brierly et al., 2019; Ning et al., 2019; Erten Taysi et al., 2019; Sharma et al., 2021).

1.2. Bone Regeneration

Bone cells are found both in the bone tissue itself and bone marrow. Bone tissue consists of osteocytes, osteoclasts, osteoblasts, pre-osteoblasts, pre-osteoclasts, and lymphoid cells.

Adipocytes, endothelial cells, mastocytes, macrophages, mesenchymal stem cells, and hematopoietic stem cells are found in bone marrow. Osteocytes constitute approximately 90% of the bone tissue and are derived from the mesenchymal stem cell line (Florencio-Silva et al., 2015).

Regeneration capability is specific to bone tissue among other body tissues (Hernandez-Gil et al., 2006). Bone is a dynamic tissue that is being absorbed and synthesized continuously. When the bone tissue gets injured, the repair process starts with an inflammatory response and is followed by bone formation and remodeling (Fraile-Martinez et al., 2021; Battafarano et al., 2021). Besides this ability, inhibited bone healing can be seen due to several reasons in clinical practice. Most of the studies investigate long bones such as tibia. Compared to other bones, the jawbone follows distinct regeneration characteristics due to its different ossification process, and mineralization density distribution (Fraile-Martinez et al., 2021). A study that compares the jawbone and tibia, concluded that the jawbone has less mass density and mineralization, and a higher remodeling rate compared to tibia (Hesse et al., 2014). Intramembranous ossification occurs in the jawbone, while endochondral ossification occurs in axial and appendicular skeletons (Omi and Mishina, 2021). The mesenchyme is directly converted to osteoblasts that are converted to bone in the process of intramembranous ossification (Breeland et al., 2023). Besides the ossification process and mineralization density, mechanical stimuli, such as continuous mastication creating microcracks, accelerate bone regeneration for protection (Iezzi et al., 2020).

1.3. Biomaterials for Bone Regeneration

Materials that are used to fix, complete, and functionalize the part of the body, as a treatment or precaution to an injury or disease, are called biomaterials (Park and Lakes, 2007). Their significant requirements are biocompatibility, pharmacological acceptability, stability, and affordable price. Different kinds of drug delivery systems such as hydrogels, films, patches, nanostructured systems, and fibers can be designed by using biomaterials (Shafiq et al., 2023; Sivasankarapillai et al., 2021; Yang et al., 2020).

Biomaterials can be composed of polymers, metals, ceramics, and composites. Polymers are mostly used in soft tissues and they may degrade over time. Hydrogels, 3D printing biomaterials, and films can be composed of polymers (Kalirajan et al., 2021). The porous

structure of polymeric biomaterials allows cells to penetrate into the biomaterial and eases the transportation of oxygen, nutrients, and waste (Boccaccini et al., 2021).

Ceramics are burnt materials that are exposed to high pressure during incineration (Desai et al., 2021). They have a high melting temperature. Although the bioceramics are fragile, their biocompatibility makes them acceptable biomaterials as permanent implants (Park and Lakes, 2007). They can be seen as an alternative to metal implants with their non-corrosive nature (Punj et al., 2021). Bioceramics are used widely in the composition of implants, scaffolds, and bone grafts. Alumina, zirconia, hydroxyapatite, and silicon nitride are some of the ceramic materials that are used in dentistry (Vaiani et al., 2023).

Metals, such as gold and cobalt-chromium alloy, are highly strong and are being used in implants, pacers, and joint replacements. They have the disadvantage of having the possibility of corrosion, which may differ from metal to metal (Chua et al., 2021).

Composite biomaterials include more than one material. Bone, skin, wood, and dentin are natural composites (Park and Lakes, 2007). Composites such as collagen-apatite (Kołodziejska et al., 2020) and chitosan-hydroxyapatite (Venkatesan and Kim, 2010) are used to mimic the bone in tissue engineering.

Material used in bone tissue engineering changes depending on the defect type and site. Defects can be caused by cancer, diseases, trauma, operation, and infection (Xu et al., 2024; Jimi et al., 2012). Designing a biomaterial for bone has similar steps compared to other tissues. Primary goals of the scaffolds are allowing nutrient flow and maintaining the proper mechanical function (Alonzo et al., 2021). Biomaterial design for bone tissue engineering requires choosing the application form, material, and manufacturing technology (Koons et al., 2020). The biomaterial can be implantable or injectable. It can be produced as particles, films, coatings, and 3D structures by using organic (polymers), inorganic (metals and ceramics), and composite materials. Proteins like collagen, gelatin, and fibrin; natural polymers like hyaluronic acid and alginate; and synthetic polymers like PNIPAM, PVA, and PEG are used in the hydrogels that are developed for mandibular bone repairing (Al Maruf et al., 2022). Additionally, metallic and ceramic nanoparticles can be added to enhance the mechanical properties. Besides hydrogels, scaffolds that consist of bioceramics, metals, and synthetic polymers including cells, bioactive ions, growth factors, cytokines, and drugs are being used to develop new biomaterials (Dec et al., 2022). A proper biomaterial for bone should enhance the cell proliferation and carry the anti-inflammatory and antibacterial properties.

Early mandibular reconstruction was mainly on autogenous bone grafts, which is still a gold standard. Nowadays, besides autogenous bone grafts, different biomaterials have been examined for mandibular tissue engineering. Stacked polymer fiber, which mimics the ECM of the bone, for the large jawbone defects was developed with the interaction of alveolar bone-like and mouse calvaria-like cells (Suzuki et al., 2022). Human bone morphogenetic protein-2 and rat adipose derived stem cells loaded hydrogels reinforced with microfibers were found to improve the angiogenic factor secretion and induce osteoclastogenesis (Ning et al., 2019).

1.3.1. Hydrogels in Tissue Engineering

Tissue engineering is a multidisciplinary field that includes biology, chemistry, physics, and clinical sciences (Hasnain et al., 2019). It deals with the biomaterials, cells, and their interaction (Radulescu et al., 2022). The aim of a tissue engineer is to develop functional structures that maintain, recover, or enhance the defective tissues with the collaboration of active molecules and cells. The need for transplantation of tissues and organs after a loss or defect due to trauma or disease encourages and brings new insights to the tissue engineering field. Biomaterials that help repair and regeneration by mimicking the extracellular matrix (ECM) and creating an environment for cell adhesion, proliferation, and differentiation are important properties in bone tissue engineering (Xu et al., 2024).

Hydrogels are polymer structured 3D crosslinked scaffolds that mimic the ECM and have the capacity of holding water. Hydrogels can be produced by using different sources and crosslinking types (Radulescu et al., 2022). They can consist of natural, synthetic, or both natural and synthetic polymers. Alginate, chitosan, and gelatin are some examples of natural polymers that are used in hydrogels (Zhang and Zhao, 2020; Rajabi et al., 2020; Lu et al.,2022). Poly(N-isopropyl acrylamide) (PNIPAM), poly (vinyl) alcohol (PVA), and polyethylene glycol (PEG) are used in hydrogels as synthetic polymers. Crosslinking types of the hydrogel can be chemical, physical, or hybrid (Bashir et al., 2020; Ho et al., 2022). Chemically crosslinked hydrogels are bonded with irreversible covalent bonds. Therefore, they are more stable than the physically crosslinked hydrogels. Small molecule, enzymatic induced, and light induced crosslinkers are used to synthesize chemically crosslinked hydrogels (Xue et al., 2022). Visible light, ultraviolet (UV), and gamma irradiation are used with the light induced crosslinking agents. Photopolymerization starts when the photoinitiator is exposed to light at a specific wavelength range. Then, depolymerization of the photoinitiator occurs and radicals are generated for radical polymerization reactions (Samadian et al., 2020). Enzymatically induced

crosslinkers are used in cellular applications because the crosslinking occurs in the biological environment, which requires specific conditions of pH and temperature (Chamkouri and Chamkouri, 2021). 1,4-butanediol diglycidyl ether (BDDE) is a chemical crosslinker agent widely used with hyaluronic acid and their hydrogels are available as commercial products (Andrede del Olmo et al., 2022). With the good quality material and application, they are considered safe. Hydroxyl groups found on hyaluronic acid form ether bonds with the BDDE via nucleophilic reaction. Similarly, during the synthesis of levan hydrogels with BDDE, primary hydroxyl groups found on hydrolyzed levan form ether bonds with epoxide groups in the basic environment (Selvi et al., 2021).

There are types of hydrogels that can be responsive to pH, temperature, and light. Hydrogels sensitive to pH are used generally in cancer treatment. The cancerous area tends to become more acidic than the healthy area due to rapid glycolysis. Thus, the drug release can be targeted to the cancerous area by using a pH responsive hydrogel (Wu et al., 2019). Polyacrylate, sodium alginate, and n-vinyl caprolactam are the polymers used to produce pH sensitive hydrogels (Zhuo et al., 2020). Temperature sensitive hydrogels are designed to be responsive to body temperature. They are in the solution state at room temperature while they turn to gel state when they are exposed to body temperature (Rafael et al., 2021). By using this feature, thermoresponsive hydrogels are used as cancer, nasal, buccal, and transdermal drug delivery systems (Yu et al., 2021). Poloxomer, PNIPAM and chitosan are some of the polymers used for developing temperature responsive hydrogels. Besides thermo- and pH- sensitive hydrogels, light sensitive hydrogels are interesting and rapid hydrogels that are suitable for 3D printers. They have good spatiotemporal control provided by the light (Sun et al., 2021). Light sensitivity is not only used for building a hydrogel, it also provides the ability to degrade the hydrogel which allows hydrogel to be implanted from the interior part of the body when it is necessary (Raman et al., 2020). Nowadays, smart hydrogels that combine these sensitive properties together are studied (Ji et al., 2020).

Hydrogels are named macro hydrogels, micro hydrogels, or nano hydrogels according to their size. Hydrogels that have particle size up to 100 nm are evaluated as nanogels (Patel and Thareja et al., 2022; Lima et al., 2020). Particle size between 100 nm and 100 μm refers to microgels while bigger particle sizes between mm and cm are named macrogels.

Size of the hydrogel matters when determining the usage area. Macrogels have an important place in pharmacy and medicine (Klein and Poverenov, 2020). They can serve as drug delivery systems, wound dressings, superabsorbents and contact lenses (Lima et al., 2020; Xu et al.,

2017). They are more suitable to use externally due to their size. Additionally, they have a place in the food industry as functional food capsules (Gheorghita et al., 2024). Microgels have the injectibility property owing to their particle size. Thus, they are used in targeted/non-targeted drug delivery and 3D printing (Dirksen et al., 2020; Campora et al., 2021; Newsom et al., 2019; Feng et al., 2022). Since they are so small, nanogels can be applied through ocular, mucosal and parenteral administration (Grimaudo et al., 2019; Wang et al., 2023). Through nanogels, the drug can be delivered to the central nervous system and targeted cells. Cancer-targeted ligand attached nanogel allows the drug to reach the overexpressed receptor on cancer cells (Guo et al., 2024). Thus, nanogel drug delivery systems can target a specific area to release the drug.

1.3.1.1. Injectable Hydrogels

Injectable hydrogels can reduce the invasiveness of the implantation process into the body or the tissue areas which are hard to reach (Overstreet et al., 2012; Rizzo and Kehr, 2021). They fill the irregularly shaped empty area easier than the non-injectable hydrogels (Ghandforoushan et al., 2023). Injectable hydrogels can be formed by shear thinning and self healing or *in situ* formation. *In situ* formation requires specific conditions to form the gel state from the sol state when they are injected to the body. They are mostly temperature or pH responsive to change the state (Ghandforoushan et al., 2023). Shear thinning and self healing injectable hydrogels disassemble during injection and recover themselves at the application area after injection (Lu et al., 2012).

Mechanical properties of the hydrogel explain its injectibility. As an important evaluation factor, rheological properties explain the injectibility and the crosslinking characteristics. Viscosity is the main parameter that describes the flow characteristic of the gel. Elastic modulus shows the stored energy and higher elastic modulus indicates a more rigid gel. Crosslinking degree, molecular weight, and concentrations can change the elastic modulus. Viscous modulus shows the resistance of the gel against the dynamic forces. Therefore, lower viscous modulus indicates that less force is required to inject the gel through the needle. Deformation resistance of the gel is indicated by the complex modulus and injectable gels show complex modulus equal to elastic modulus (Alonso et al., 2021). Lower viscosity, elastic modulus and viscous modulus together indicate an easier injection of the gel (Stojkov et al., 2021).

1.4. Levan

Levan is an amphiphilic exopolysaccharide that composed of a glucose and β-2,6 linked fructosyl residues (Figure 1.1) (Toksoy Oner et al., 2016; de Siquera et al., 2020). It is synthesized by plants and microorganisms in nature by converting sucrose. Production of levan can be done enzymatically or microbially and it makes a difference in some features of levan such as degree of branching, molecular weight and adhesive strength. Genera of *Bacillus*, *Aerobacter*, *Lactobacillus*, *Zymomonas*, *Halomonas*, *Erwinia*, *Pseudomonas*, and *Streptococcus* are known as levansucrase producing bacteria (Srikanth et al., 2015; Toksoy Oner et al., 2016; Tomulescu et al., 2016).

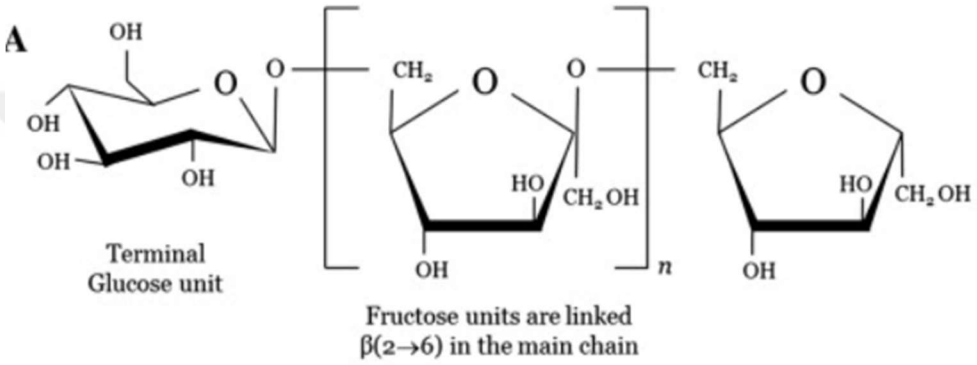

Figure 1.1. Chemical structure of linear levan (Toksoy Oner et al., 2016)

Levan polysaccharide has various characteristics suitable to be used as a component of a biomaterial. Non-toxicity, biodegradability, biocompatibility, anticoagulant, anti-inflammatory, immunostimulant and antioxidant activities, and cost effectiveness are some of the features of levan that makes it a favorable polymer (Kırtel and Combie, 2022; Erginer et al., 2016). It has application areas in pharmaceutics, cosmetics, and food with these characteristics (Toksoy Oner et al., 2016). Besides levan alone, it was studied in different kinds of biomaterials such as films and hydrogels for drug delivery. Its self assembly property allows it to form nanoparticles. PLGA and levan combined curcumin carrying nanoparticle formulation showed stability for at least 3 months (Eskandari et al., 2021). Edible films for packaging were designed by taking the advantage of oxygen impermeability of levan films and being adhesive (Gan et al., 2022; Toksoy Oner et al., 2016; De Siqueira et al. 2020).

1.4.1. *Halomonas* Levan

Halomonas smyrnensis is a gram negative, halophilic bacterium isolated from the Çamaltı Saltern area (Poli et al., 2013). It is the first known levan producer as an extremophile (Poli et

al., 2009). Being halophilic provides an advantage to be able to be cultured at non-sterile conditions (Toksoy Oner et al., 2016). *Halomonas* levan and its derivatives were studied to explore their effects. Besides this, multilayer/blend films, hydrogels, and nanoparticles were synthesized and characterized (Costa et al., 2013; Sima et al., 2012; Bostan et al., 2014; Sezer et al., 2011; Cinan et al., 2021; Selvi et al., 2021). In-vitro anticancer activity of *Halomonas* levan was observed with the oxidation of the polymer (Sarilmiser and Toksoy Oner, 2014). Sulphated levan with the increasing degree of sulfation showed anticoagulant activity (Erginer et al., 2016). Levan and levan derivatives (sulfated and hydrolyzed) showed activities that enhance the skin barrier function, and proved that they can be used in cosmeceutical formulations with their ability to enhance the production of hyaluronic acid and collagen (Erginer et al., 2023). Poly(caprolactone) nanofiber supported with sulfated levan, that shows better proliferation, migration, and cell adhesion, was designed to be used for curing the defects of tympanic membrane (Akgul et al., 2024). Electrosprayed biocompatible nanoparticles were formed with *Halomonas* levan as a drug delivery system (Cinan et al., 2021). Another levan nanoparticle had been studied to show that they are suitable for drug delivery of proteins (Sezer et al., 2011). Hydrogels synthesized with levan (Demirci et al., 2020) and levan derivatives (Selvi et al., 2021) were investigated for their adhesiveness and controlled drug release.

1.5. Cannabidiol (CBD)

Cannabidiol (CBD) is a hydrophobic cannabinoid compound of the plant *Cannabis sativa* together with the nearly 80 other cannabis compounds (Ghasemi et al., 2022; Baines et al., 2024). It is used in the treatment of cancer, and neurodegenerative disorders (Heider at al., 2022; Bhunia et al., 2022). CBD is a non-psychoactive compound and has antioxidant, pain-killer, anti-diabetic, anti-nausea, anti-inflammatory, and anti-cancer activity properties (Pisanti et al., 2017; Morakul et al., 2023). In an in vitro study, increased wound closure area of gingival fibroblast cells was observed in the presence of CBD (Kongkadee et al., 2022). CBD was investigated in terms of oral wound healing and showed an antiinflammatory effect in the early days of the *in vivo* wound healing process (Klein et al., 2018).

CBD interacts as a ligand with the human endocannabinoid system which includes receptors, ligands and enzymes (Peng et al., 2022). Main cannabinoid receptors are called cannabinoid receptor type 1 (CB1) and cannabinoid receptor type 2 (CB2). CB1 is a G-protein-coupled receptor expressed in the central nervous system, adipocytes, musculoskeletal tissues, hepatocytes, and connective tissues (Bridgeman and Abazia, 2017). Activation of this receptor

leads to decreased bone formation inhibition through decreasing of norepinephrine (Clouse et al., 2022). CB2 receptors are expressed in the immune system related cells. Moreover, CB2 was found related to osteoporosis in women (Clouse et al., 2022).

1.6. Aim of this thesis

Cannabidiol (CBD)-loaded *Halomonas* levan hydrogels were investigated in this thesis for their potential to prevent medication-related osteonecrosis of the jaw (MRONJ). The study hypothesized that levan-based hydrogels would enhance the proliferation of human osteoblast (HOB) cells and enable a controlled release of CBD at non-toxic concentrations without an initial burst release. Considering the importance of tissue-material interaction, the development of a hydrogel capable of filling irregularly shaped cavities and promoting bone cell proliferation was targeted. To this end, 1:25, 1:30, and 1:35 *Halomonas* levan hydrogels were synthesized and characterized through swelling, stability, and gel fraction tests. For application feasibility, the hydrogels were shredded to evaluate their injectability.

Release studies were performed to assess the drug release profile, while cell viability assays with HOB cells were conducted using lyophilized hydrogels in bulk and ground forms, as well as hydrogel extracts, to evaluate their cytocompatibility. Unlike other hydrogels studied for MRONJ in the literature, as discussed in Section 1.1, the incorporation of CBD into ground *Halomonas* levan hydrogels introduces a novel approach to addressing this clinical challenge. This study revealed that these hydrogels demonstrated appropriate swelling behavior, controlled CBD release, and biocompatibility, offering new insights into potential therapeutic strategies for MRONJ.

2. MATERIALS AND METHODS

2.1. Materials

2.1.1. Chemicals

Chemicals that were used in the medium of levan production were supplied from MERCK (Germany) and Sigma (USA). Salt from Çamaltı, İzmir saltern area (provided by Estuz company) was used in substrate solution of the enzymatic levan production. CBD was provided from CBD.epot (Czech Republic). PBS tablets were purchased from MP biomedicals. Abbkine CCK-8 was used for cell viability tests. DMEM, FBS and antibiotics were provided from PAN Biotech (Germany).

2.1.2. Equipment

Equipment used in the experiments were listed in Table 2.1.

Table 2.1. Equipment list

Equipment	**Brand**
Autoclaves	Nüve OT32V S, Biolab Systec 3870
Magnetic stirrers	Heidolph Mr3003s, Heidolph MR3001 K
Refrigerators	+4 ℃ Arçelik, +4 ℃ Beko
Freezer	-20 ℃ Arçelik, -20 ℃ Beko, -80 ℃ Thermo Fischer Scientific
Shaker incubators	Certomat BS1, New Brunswick Scientific Excella E24
CO_2 Incubator	Thermo Scientific Steri-cycle CO_2
Drying Oven	Binder Ed115
Biosafety cabinets	Nüve MN090, Thermo Scientific MSC Advantage
Light microscopy	SOIF XDS-1B
Centrifuges	Hermle/Z36HK, Nüve/NF800, Nüve/NF 4000R,
Precise vacuum oven	Visd TermoStable OV-30
Lyophilizer	Christ Freeze Dryer, Alpha 1-2 LDplus
Spectrophotometer	5100 UV-VIS Spectrophotometer
Automatic micropipette sets	4500080 Finnpipette, 4500110 Finnpipette
Sonicator	Bandelin Sonopuls HD 4200
Blender	Fakir stor stick
Grinder	Kiwi KSPG-4820
Homogenizer	Heidolph DIAX900
pH meter	Mettler Toledo MP 220
Zetasizer	Malvern Zetasizer Nano ZS90

2.2. Methods

2.2.1. Production and Purification of Levan

Production of levan was performed by following the procedure from Kirtel et al. (2018). LB medium was prepared with sodium chloride (NaCl), peptone from casein, and yeast extract. *E.coli* BL21DE3, which contains levansucrase gene from *H. smyrnensis*, was subcultured in the kanamycin added 10 ml LB media at 37℃ and 180 rpm. 1% inoculation was done into 200 ml media when the OD reaches 0.6-0.8 at 600 nm. IPTG was added to the media for gene expression when the culture reached the target turbidity. Cultures were incubated at 26 ℃ overnight. Next day, the culture was centrifuged at 4℃, 8000 rcf for 20 minutes and the cell pellets were dissolved in the 6.6 pH phosphate (cell lysis) buffer that contains KH_2PO_4, K_2HPO_4, and NaCl. Sonication was applied to the mixture at 30% power for 15 minutes. After sonication, the mixture was centrifuged at 8000 rcf for 20 minutes and the pellet was discarded. Immobilized metal affinity chromatography (IMAC) was prepared with a 10 CV equilibrium buffer (7.4 pH). Supernatant was mixed with the equilibrium buffer with 1:1 ratio and passed through the column. 10 CV wash buffer (7.4 pH) was passed through the column after the crude enzyme to collect the protein impurities. After the wash buffer, 10 CV elution buffer (7.4 pH) was passed through the column to cut the histidine tag and collect the target protein. Substrate was prepared with KH_2PO_4, K_2HPO_4, sucrose, and salt from the Çamaltı saltern area. 2 liters of substrate was passed through Whatman paper filter and 0.5 M EDTA was added to the solution. Pure enzyme was mixed with 5.9 pH substrate and incubated at 15 ℃ overnight. Next day, 2:3 ethanol was added for the precipitation and left overnight in -20℃. After the clear ethanol was discarded with the help of a peristaltic pump, the precipitate was collected with centrifugation at 4℃, 8000 rcf, for 20 minutes and dissolved in distilled water. The levan mixture was put into dialysis tubes and dialyzed for a couple of days to eliminate the salt impurities. DEAE Sepharose weak ion exchange column was used to get rid of the protein impurities. Levan was dried at 50℃ and crushed for further use.

2.2.2. Hydrolysis of Levan

Hydrolysis of levan was performed by using a method from Avsar et al. (2018) with a slight change. 10 g of levan was dissolved in 171.5 ml of distilled water. 3.5 ml of acetic acid was added and left for hydrolyzation for 10 minutes. Then, the solution was put into a microwave at 60% power. Every 30 seconds, a diluted sample from the solution was taken and its OD was measured at a spectrophotometer until reading A_{600} = 0.1-0.06 indicating the disruption of secondary structures and associated lowering of the turbidity. At every interval, the solution

was cooled in an ice bath. Three times the volume of ethanol was added onto the hydrolyzed levan and left overnight in the freezer. Next day, the precipitated hydrolyzed levan was collected with centrifugation at 8000 rcf for 30 minutes. It was dried in a vacuum oven at 45°C for 24 hours and stored at -20°C. For structural characterization, FTIR (Fourier-transform Infrared Spectroscopy) analysis was performed between 600-4000 cm^{-1} with Thermo Scientific Nicolet 6700 equipment while for the molecular weight, GPC (Gel Permeability Chromatography) analysis with TOSOH EcoSEC HLC-8320 was performed.

2.2.3. Synthesis of Levan Hydrogels

The protocol from Selvi et al. (2021) was followed with slight difference to produce the levan hydrogels. Briefly, 7% (w/v) hydrolyzed levan was dissolved in 0.25 M NaOH solution and mixed with BDDE for an hour on the magnetic stirrer with the ratios of 1:25, 1:30, and 1:35 in a 24 well plate. The plate was placed into a 55°C water bath overnight. Next day, the hydrogels were collected from the plate and washed with distilled water for 3 days by refreshing the water 2 times a day. They were air dried at 55°C for a day and stored at 4°C until further use. FTIR analysis was used for structural characterization. .

2.2.4. Swelling Test

1:25, 1:30, and 1:35 levan hydrogels' swelling was examined under different pH (5.0, 7.4, and 9.0) and temperature (15°C, 35°C, and room temperature) conditions. Acetate buffer as pH 5.0 buffer, PBS as pH 7.4 buffer, and boric buffer as pH 9.0 buffer were used for the swelling test. Acetate buffer (pH 5.0) was prepared with 2.886 g sodium acetate and 0.845 ml acetic acid dissolved in distilled water. Its pH was adjusted by adding HCl. PBS (Phosphate buffered saline, pH 7.4) was prepared by dissolving the PBS tablets in distilled water with 1X concentration. Boric buffer (pH 9.0) was prepared with 6.2 g boric acid dissolved in distilled water and its pH was adjusted by adding NaOH solution.

Dry hydrogels were weighed (W_d). Hydrogels were soaked into 3 ml of buffers and left in the incubator at 37°C. Every 30 minutes until 3 hours, the excess buffer was removed, hydrogels were weighed (W_s), and a fresh buffer was added for the next measurement. The hydrogels were weighed after 24 hours, 48 hours, and 72 hours, too. The experiment was repeated at 15°C, 37°C, and room temperature with PBS. The swelling degree (g/g) was calculated according to the equation below (Selvi et al., 2021).

$$\text{Swelling degree (g/g)} = W_s/W_d$$

2.2.5. Gel Fraction Test and Stability

The experiment was carried by following the procedure from Halligan et al. (2023) with slight differences. Dry 1:25, 1:30, and 1:35 levan hydrogels (G_i) were weighed and left in the distilled water for a day. Swollen hydrogels were air dried at 50°C for 24 hours and weighed (G_f). Gel fraction percentage was calculated according to the equation below.

$$\text{Gel fraction (\%)} = (G_f/G_i)\times 100$$

The test was repeated two times more with the whole hydrogels to observe the gel content change and the stability with repeated swelling and drying process. Images of dry 1:35 hydrogels were taken at every repetition.

2.2.6. Shredding the Hydrogels and Z-average and PdI measurements

1:25, 1:30, and 1:35 hydrogels were shreded with different equipment. Grinder, homogenizer, blender, and sonicator were used to obtain smaller sizes of the hydrogels. The size and the polydispersity of the hydrogels were examined with DLS (dynamic light scattering) method. Sonicator was used after every equipment to decrease the value of polydispersity index (PdI).

2.2.6.1. Grinder and Sonicator Shredded Hydrogels

Dry hydrogels (1:25, 1:30, and 1:35) that were ground for 30 seconds in the grinder were swollen in distilled water for 3 days. Swollen hydrogels were sonicated with 30% power for 4 minutes with 30 seconds intervals between 1 minute of sonication. After sonication, the samples were centrifuged for 10 minutes at 2000 rcf. Size and PdI of the hydrogels were analyzed.

2.2.6.2. Homogenizer and Sonicator Shredded Hydrogels

1:35 hydrogel with the volume of 35 ml was put into 200 ml of distilled water and shredded with the homogenizer for 5 minutes with 30 seconds of intervals every 1 minute. The mixture was centrifuged for 10 minutes at 2000 rcf. The pellet was dispersed in distilled water that completes the volume to 50 ml and sonicated with 30% power for 16 minutes with 30 seconds intervals between 1 minute of sonication. At the end of the first 4 minutes, the mixture was centrifuged at 2000 rcf for 10 minutes. Supernatant was collected and the pellet was dispersed in distilled water again and sonicated for another 4 minutes. The mixture again centrifuged under the same conditions. Supernatant collected and the pellet dispersed in distilled water was

sonicated for 8 minutes. For the size and PdI measurement, the pellet sample was dispersed in the distilled water with the diluted concentrations (100, 50, 25, 10, 5, and 2.5 mg/ml).

2.2.6.3. Blender and Sonicator Shredded Hydrogels

1:35 hydrogel with the volume of 35 ml was put into 100 ml of water and exposed to 1000 W blender for 5 seconds. The mixture was centrifuged for 5 minutes at 2000 rcf. 10 g of pellet was dispersed in distilled water that completes the volume to 40 ml. The mixture was sonicated with 30% power for 4 minutes with 30 seconds intervals every 1 minute. The mixture was centrifuged with the same conditions and pellet was again dispersed in distilled water. The mixture was again sonicated and centrifuged. Samples from supernatant, pellet and mixture of supernatant and pellet were taken for the measurement of size and PdI.

2.2.7. CBD Release Test

1:35 hydrogels were ground for 30 seconds in the grinder and 0.6 g of the hydrogel was put into a 50 ml falcon tube. 20, 50, and 243 mg/ml CBD/EtOH solutions were prepared and 0.6 ml of the solution was added onto the hydrogel. Total volume of the liquid was completed to 12 ml with distilled water and left for swelling for 5 days on the magnetic stirrer. Thus, the final concentrations were calculated as 1, 2.5, and 12.15 mg/ml. At the end of the fifth day all the liquid was soaked by the hydrogels. 1 ml of hydrogel was placed into the dialysis tube with the help of a syringe. The dialysis tube was placed into a falcon tube that contains 20 ml of 5% (v/v) EtOH/PBS releasing medium and incubated at 100 rpm, 37℃. For 3 hours, every 15 minutes 1 ml sample was taken from the medium and replaced with a fresh medium. Samples at 24th, 48th, and 72nd hours were taken. CBD concentration was measured by using the Beam test (Sosnik et al., 2021). 5% (w/v) KOH in ethanol was prepared for the Beam test. It was added onto the samples at 1:1 ratio and incubated at 100 rpm. OD was measured at 274 nm by using a UV/vis spectrophotometer. Cumulative release concentrations were calculated by summing the concentration of each sample with the concentrations of the samples before.

2.2.8. Cell Viability Tests

Human Osteoblast (HOB) cell line was used for the cell culture experiments. Cell viability tests of lyophilized levan hydrogels (ground and bulk), oven dried levan hydrogels (extract) and CBD/EtOH in different concentrations were performed.

HOB cell line was taken from the -80℃ stock and thawed with 37℃ DMEM medium. Freezing medium was discarded after centrifugation and the cell pellet was dispersed in the fresh

medium. The cells were seeded to T25 flasks and incubated at 37°C and 5% CO_2. When the cells reach confluency, medium was discarded and the cells were washed with PBS solution. Trypsin was added onto the cells, for detachment of the cells from the surface. Fresh media was added to stop the trypsin activity and the cells were centrifuged. Cell pellet was dispersed in the fresh medium and 50 µl sample was mixed with 1:1 4% (w/v) trypan blue in PBS solution. Alive cells were counted with a hemocytometer and calculated according to the equations below.

$$\text{Cell concentration} = \text{Number of the counted cells} \times \text{dilution factor} \times 10^4$$

$$\text{Total cell number} = \text{Cell concentration} \times \text{Cell suspension volume}$$

After counting the cells, they were seeded to the 96 well plates for the experiments.

2.2.8.1. Cell Viability Test of Levan Hydrogel Extracts

Oven dried 1:25, 1:30, and 1:35 hydrogels were sterilized by exposing UV light for 1 hour for each side and left in DMEM for 24, 48, and 72 hours to obtain the extracts. 10^4 cells/well was seeded to a 96-well plate and next day, the media were discarded and the extracts were added onto cells. After 24 hours of incubation at 37 °C and %5 CO_2, the CCK-8 kit was applied according to the kit instructions. CCK-8 was mixed with fresh medium and extracts were replaced with the CCK-8. At the end of the 2 hours incubation (at 37°C, 5% CO_2), OD measurement was done at 450 nm.

2.2.8.2. Cell Viability Test of Lyophilized Levan Hydrogel Pieces

Hydrogels that were swollen with distilled water were cut with a biopsy punch and dried with lyophilization. They were sterilized under UV light for 1 hour for each side and placed to the wells of the 96-well plate. 10^4 cells/well was put onto hydrogels. Since the media were soaked by the hydrogels, 150 µl fresh media were added to the wells. Cells were incubated for 24, 48, and 72 hours at 37°C, 5% CO_2. Each day, the CCK-8 kit was applied and OD measurement was done at 450 nm.

2.2.8.3. Cell Viability Test of Ground Lyophilized Levan Hydrogels

Lyophilized 1:25, 1:30, and 1:35 hydrogels were ground and sterilized under UV light for 2 hours. Hydrogels were mixed with fresh medium and placed (100 µl) in the wells of a 96-well plate. 10^4 cells/well were added onto hydrogels and incubated for 24, 48, and 72 hours at 37°C,

5% CO_2. After 24 hours, CCK-8 was added to the wells and incubated for 2 hours. OD measurement was done at 450 nm. It was repeated at 48th and 72nd hours.

2.2.9. Statistical Analysis

One-way ANOVA and Tukey tests of the results were performed by using software (GraphPad Prism 8.0) to interpret the data.

3. RESULTS AND DISCUSSION

3.1. FTIR Analysis

Hydrogels were synthesized by crosslinkinng hydrolyzed levan polymers with BDDE as described in section 2.2.3 and then subjected to several characterization tests. FTIR analysis was performed for structural characterization of hydrolyzed levan (Figure 3.1.) and 1:25, 1:30, and 1:35 BDDE crosslinked levan hydrogels (Figure 3.2.). Hydrolyzed levan showed the characteristic peak around 3200 cm^{-1} (indicating -OH stretch) that proves the existence of fructofuranoses (Erginer et al., 2016). The peak around 2850 cm^{-1} (indicating C-H stretch) shows the fructose residues of hydrolyzed levan. Increasing intensities of the peaks at 1050-1150 cm^{-1} (indicating C-O-C stretch) and 2800-2950 cm^{-1} (indicating C-H stretch) show the stable ether bonds between the polysaccharide and the crosslinker (Andrade del Olmo et al., 2022; Selvi et al., 2021). Decreasing peak intensity between 800-900 cm^{-1} (indicating C-O stretch) shows the disappearance of the epoxy ends of BDDE due to crosslinking reactions (Andrade del Olmo et al., 2022). Mentioned peak intensity changes at the specified ranges were observed to be directly proportional to the BDDE concentration of the hydrogels.

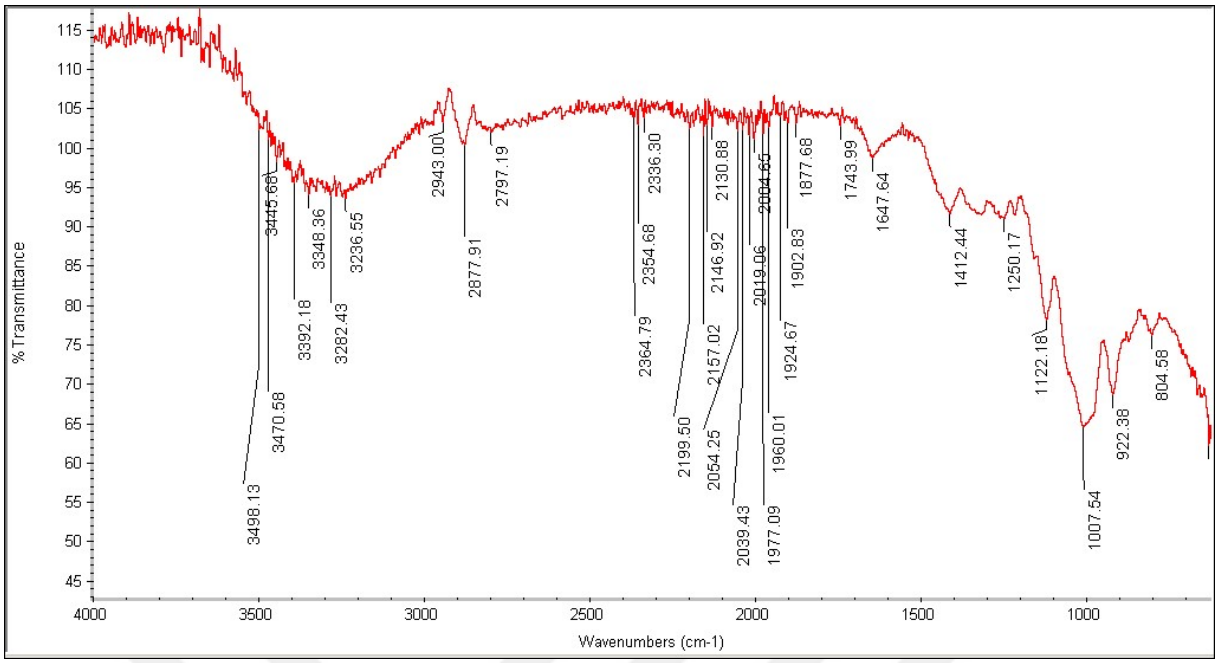

Figure 3.1. FTIR graph of hydrolyzed levan

A.

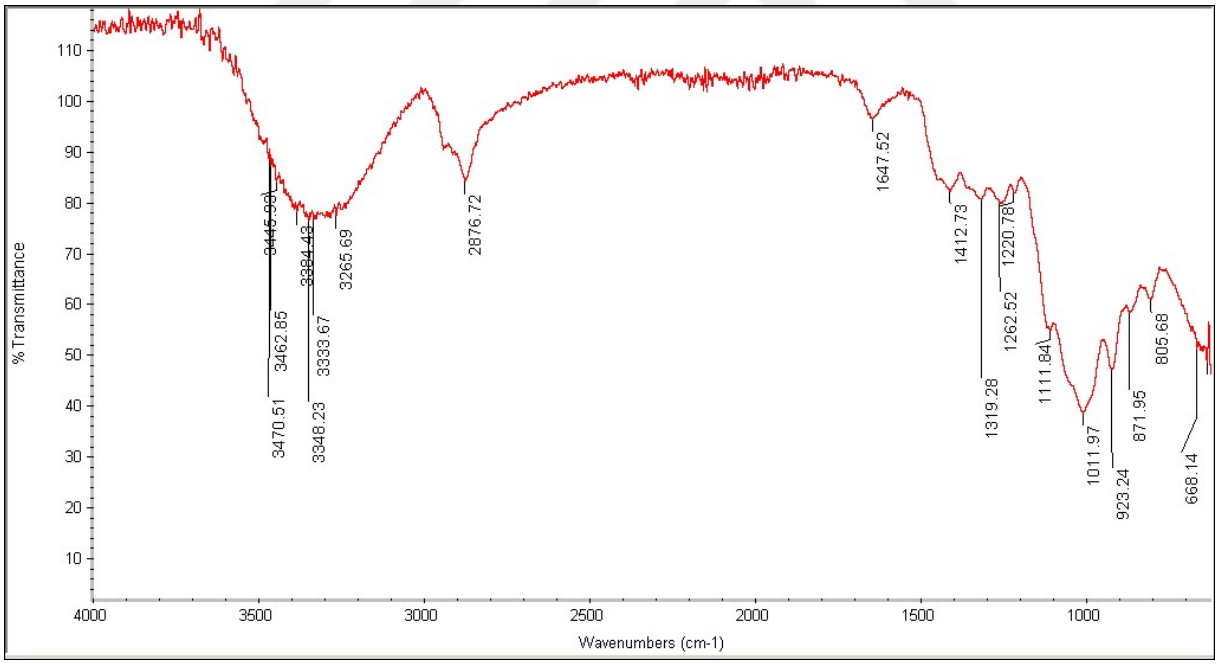

B

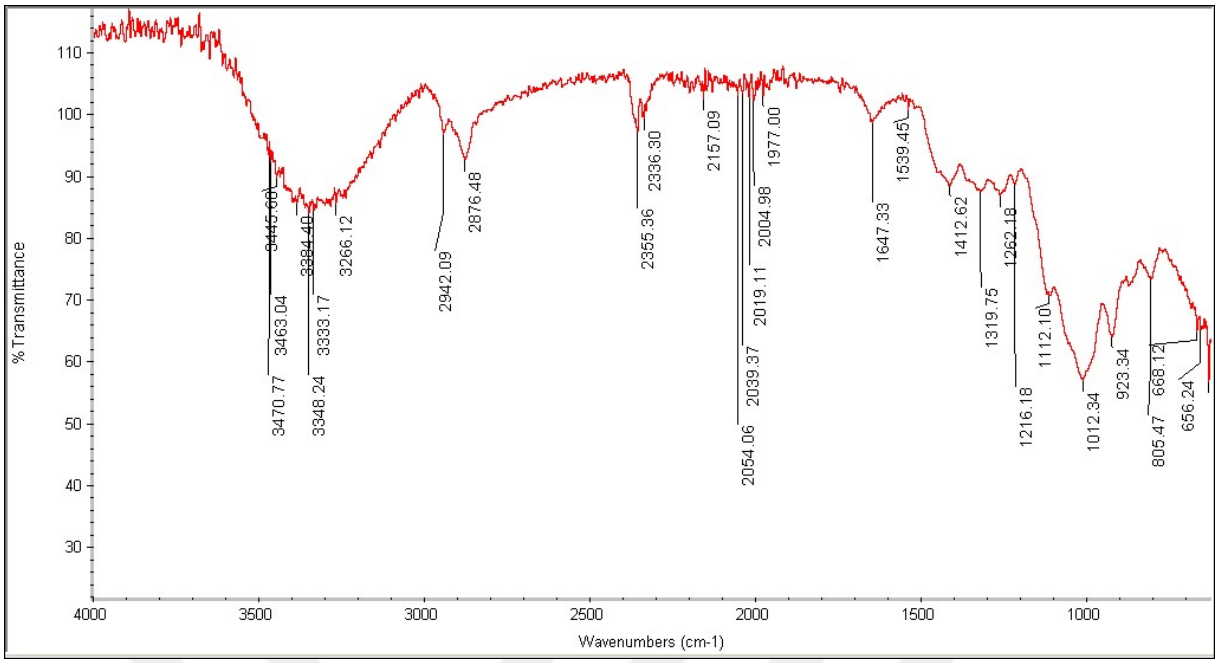

C

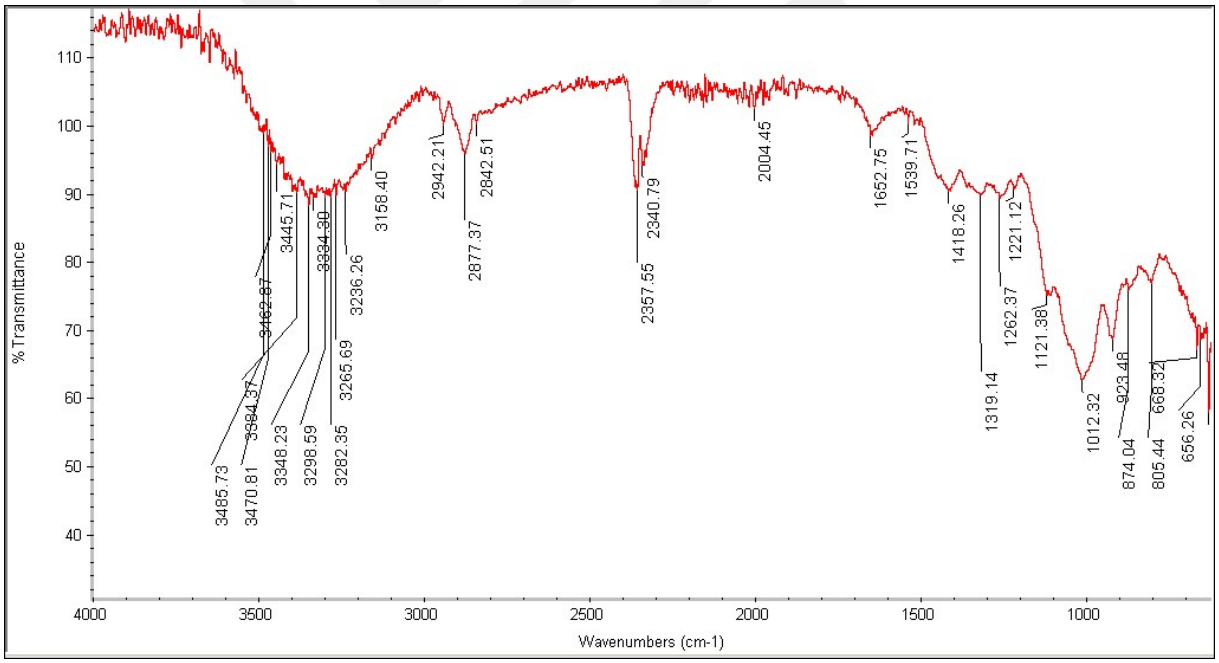

Figure 3.2. FTIR graphs of 1:25 (A), 1:30 (B), and 1:35 (C) BDDE crosslinked levan hydrogels

3.2. GPC Analysis

The number average molecular weight and weight average molecular weight of levan and hydrolyzed levan were given in Table 3.1. A decreased molecular weight of levan was observed after the hydrolyzation process.

Table 3.1. Molecular weights of levan and hydrolyzed levan according to GPC results

	Molar mass moments (Da)	Peak 1	Peak 2
Levan	M_n	1.364×10^6	
	M_w	1.499×10^6	
Hydrolyzed levan	M_n	1.662×10^6	4.813×10^5
	M_w	1.784×10^6	5.355×10^5

3.3. Swelling Test

Evaluating the swelling behavior of a hydrogel in different pH and temperatures is important in terms of understanding how the hydrogel swells or shrinks when applied to different parts of the body (Tran Vo et. al., 2022). Therefore, a swelling test was applied to the levan hydrogels to examine the response of the levan hydrogel in acidic, basic, neutral, cold, room temperature, and body temperature. When the hydrogels swell in a narrow range of pH or temperature they are called pH sensitive or temperature sensitive and it affects impact of the loaded drug. Developing temperature sensitive hydrogels is possible by using temperature sensitive polymers like Poly(N-isopropylacrylamide) (PNIPAM) (Hu et al., 2022; Ayar et al., 2021). When developing pH sensitive hydrogels, charge of the hydrogels is important. Anionic hydrogels swell in high pH media, while cationic hydrogels swell in low pH media (Rizwan et al., 2017). Swelling behavior of 1:25, 1:30, and 1:35 levan hydrogels was examined under 37°C basic (boric buffer, 9.0 pH), neutral (PBS, 7.4 pH), and acidic (acetate buffer, 5.0 pH) conditions (Figure 3.3.). Further, the experiment was repeated under 37°C, room temperature, and 15°C. Highest swelling degree was measured with 1:35 hydrogels at 37°C, boric buffer as 18.96 g/g. However, after 3 days of swelling, regardless of the pH and the temperature, no significant weight difference was observed among all hydrogels. Moreover, pH or temperature sensitivity was not detected. When the saliva pH (6.8-7.8) (Uchida and Ovitt, 2022) was considered, the 37°C PBS buffer is the best mimicking medium for the target area. At that condition, the highest swelling degree was observed with the 1:35 levan hydrogel, which

contains the least amount of chemical crosslinking among the hydrogels. Thus, 1:35 levan hydrogel was considered more convenient for the further tests.

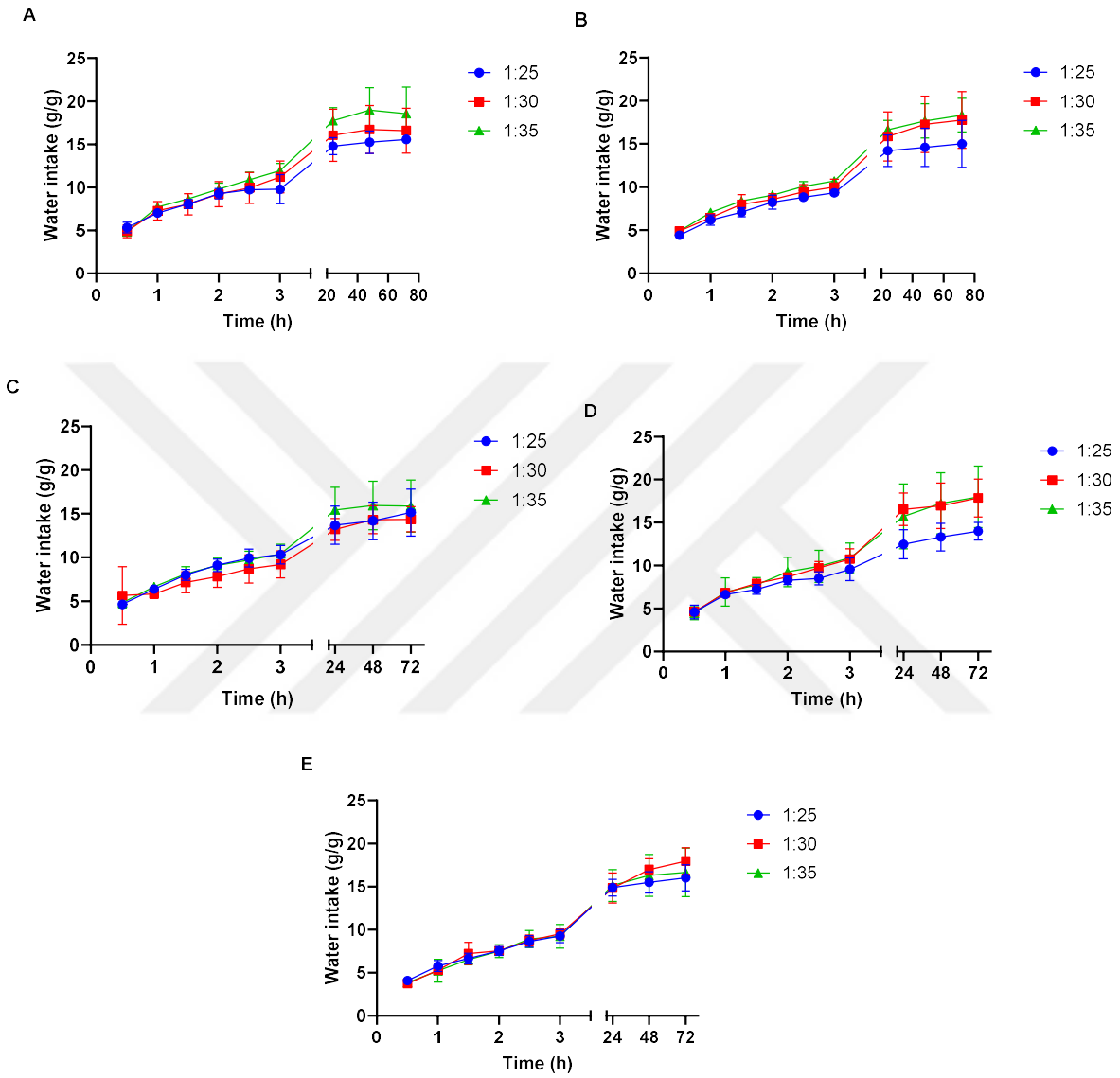

Figure 3.3. Graphs of hydrogels at different temperature and pH until 72nd hour. A. 9 pH 37℃ B.5 pH 37℃ C. 7.4 pH 37℃ D. 7.4 pH room temperature E. 7.4 pH 15℃

Highest swelling degrees at the end of 72 hours was obtained as shown in the table 3.2..

Table 3.2. 72 hours swelling degrees (g/g) of the hydrogels in 9 pH 37℃, 5 pH 37℃, 7.4 pH 37℃, 7.4 pH room temperature, and 7.4 pH 15℃.

	Highest swelling degree of the hydrogels (g/g)		
	1:25	**1:30**	**1:35**

9 pH, 37 ℃	15.56	16.72	18.96
5 pH, 37℃	15.01	17.78	18.35
7.4 pH, 37℃	15.14	14.36	15.95
7.4 pH room temperature	14.00	17.87	17.98
7.4 pH 15℃	16.03	17.97	16.64

Change in the polymer chain structure can alter the swelling ratio of the physical hydrogels (Yang et al., 2012). It is known that microbial *Halomonas* levan is not branched while enzymatic *Halomonas* levan has 10% branching (Kirtel et al., 2019). 1:20 microbial *Halomonas* levan hydrogels with BDDE crosslinker were swollen with PBS at 37 ℃ and 5.095 swelling degree was recorded (Selvi et al., 2021). By comparing these results, it can be speculated that the difference in the concentration and the production method of the levan can alter (increase in this case) the swelling degree.

3.4. Gel Fraction Test and Stability

Gel fraction of 1:25, 1:30, and 1:35 whole hydrogels was calculated as 93.93%, 95.97%, and 100.26% respectively (Figure 3.4.). After repeated swelling and drying of the same hydrogels, 89.42%, 93.08%, and 99.36% gel fraction was obtained for 1:25, 1:30 and 1:35 hydrogels respectively. For the third repeat, the gel fraction was calculated as 86.57%, 91.92%, and 101.3%, respectively in the same order. As the repeat number was increased, the gel fraction difference between the hydrogels was increased. In the literature, lower gel fraction indicates the less flexibility and weakness as a general behavior of the hydrogels (Kim et al., 2008). Therefore, 1:25 hydrogels were found less easy to bend compared to 1:35 hydrogels. As the flexibility decreases, the hydrogels tend to be broken apart as they are exposed to repeated swelling and drying. Additionally, the pattern between the different concentrations allows to comment that the increased levan concentration increased the gel fraction by increasing the crosslinking.

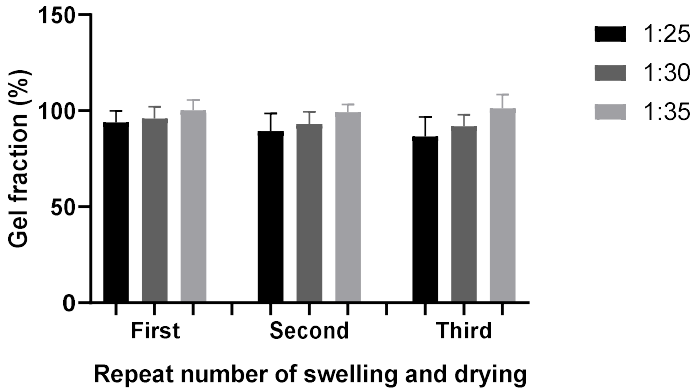

Figure 3.4. Repeated gel fractions of 1:25, 1:30 and 1:35 hydrogels.

Images were taken after every drying step to observe the 1:35 hydrogel stability. Increased disintegration and deterioration in form was observed during the repeated process of swelling and drying (Figure 3.5.).

Figure 3.5. 1:35 hydrogel forms after the first, second, and third repetition of the swelling and drying process respectively from left to right.

Gel fraction for the ground 1:25, 1:30, and 1:35 hydrogels were calculated as 78.55%, 85.6%, and 84.24%, respectively (Figure 3.6.).

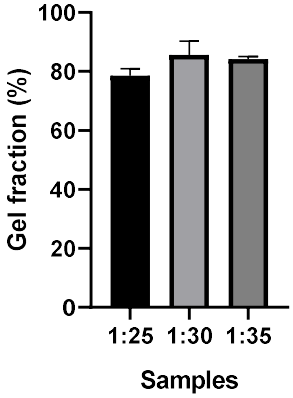

Figure 3.6. Gel fraction of ground 1:25, 1:30, and 1:35 hydrogels

Gel fraction of a hydrogel defines the covalent bond number between the polymer and the crosslinker (Halligan et al., 2023). Lower gel fraction was observed for ground hydrogels compared to non-ground hydrogels. Broken bonds as a result of the grinding process can be shown as a reason for this decrease.

3.5. Z-average and PdI measurements of the Shredded Hydrogels

Increasing the surface area by breaking the hydrogels into pieces, thus, increasing the CBD absorption into the hydrogel was aimed. The hydrogel was also tried to be made injectable by shredding with a grinder, sonicator, blender, or homogenizer. Monodispersed, homogenous, and injectable drug delivery system was aimed by measuring the polydispersity index (PdI) and particle size of the shredded hydrogels. PdI of a mixture defines the particle size distribution of dispersed particles (Mahbubul, 2018). As the PdI value approaches to 1 from 0, the particle size diversity increases. Therefore, if the PdI value is 0 (or close to 0), the suspension is defined as monodisperse.

Particle size of the microgels are measured with micrometers, while the nanogels are measured smaller than 100 nm (Patel and Thareja, 2022). Nanogels are distinguished from microgels with their possible ability to pass through the hardest barriers of the body due to their size. Moreover, nanogels can be carried through mucosal pathways (Duan et al.,2023). Nano hydrogels are prone to be used as an internal organ targeted drug delivery system with these features. Hydrogels were shredded by using a grinder, homogenizer, blender, and sonicator. The hydrogel particle sizes measured in the scope of this thesis were measured bigger than nano and high polydisperse mixtures were obtained.

3.5.1. Grinder and Sonicator Shredded Hydrogels

Dry hydrogels were shredded in the grinder and swollen to sonicate. Particle size and PdI of the supernatant were measured with dynamic light scattering (DLS) method. Particle size of the levan hydrogels with different BDDE concentrations was measured as 339 d.nm for 1:25, 385 d.nm for 1:30, and 342 d.nm for 1:35 (Figure 3.7.A.). PdI values were recorded as 0.301 for 1:25, 0.304 for 1:30, and 0.311 for 1:35 (Figure 3.7.B.).

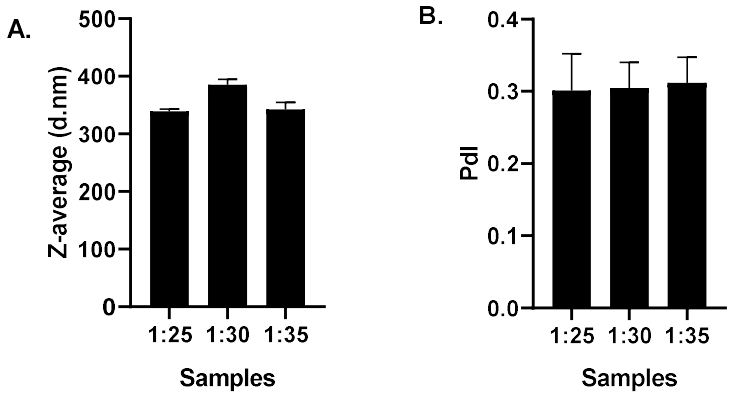

Figure 3.7. A. Z-average of the hydrogels shredded with grinder and sonicator B. PdI of the hydrogels shredded with grinder and sonicator

3.5.2. Homogenizer and Sonicator Shredded Hydrogels

1:35 hydrogel shredded with homogenizer and sonicator. Size of the particles and PdI in the supernatant was measured as 342 d.nm and 0.399 (Figure 3.8.). Z-average of the pellet was measured as 5283 d.nm for 100 mg/ml, 5820 d.nm for 50 mg/ml, 3039 d.nm for 25 mg/ml, 1472 d.nm for 10 mg/ml, 1734 d.nm for 5 mg/ml, and 1607 d.nm for 2.5 mg/ml (Figure 3.8.A.). PdI value was measured as 0.352 for 100 mg/ml, 0.322 for 50 mg/ml, 0.927 for 25 mg/ml, and 1 for 10, 5, and 2.5 mg/ml (Figure 3.8.B.). Pellet was diluted to overcome the aggregation formation. As the pellet was diluted the particle size decreased, however the dispersion went far away from being monodisperse. It showed a broad molecular weight distribution which indicates that it was heterogeneous and might not be able to release the active ingredient equally.

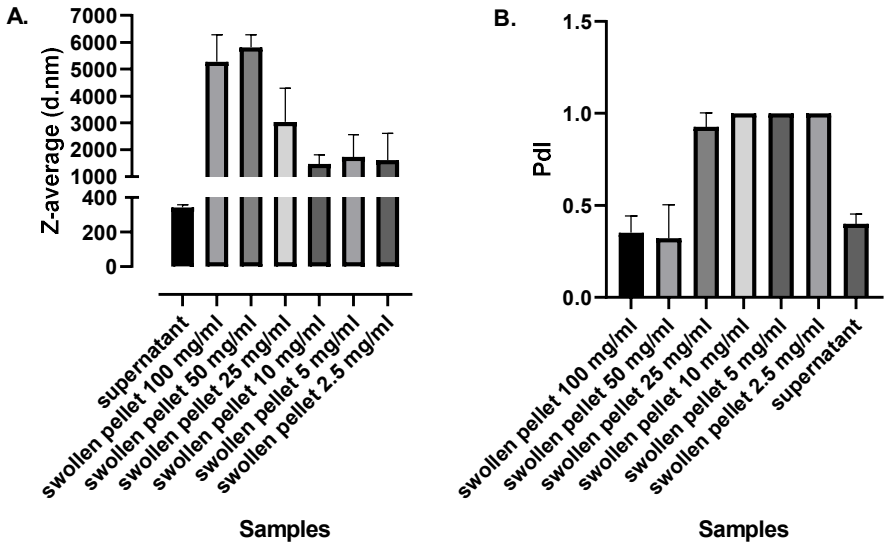

Figure 3.8. A. Z-average of 1:35 hydrogels shredded with homogenizer and sonicator B. PdI of 1:35 hydrogels shredded with homogenizer and sonicator

3.5.3. Blender and Sonicator Shredded Hydrogels

Z-average and PdI values of 1:35 hydrogels shredded with blender and sonicator was shown in Figure 3.9. and 3.10., respectively. Particle size of the hydrogel blended for 5 seconds was measured as 1266 d.nm. After centrifuge, the particle size in the supernatant was measured as 342 d.nm. For these two measurements PdI was recorded as 0.904 and 0.503, respectively. Pellet was diluted to 100, 50, 25, 12.5, and 6.25 mg/ml and particle sizes were measured as 1058, 1156, 1611, 1665, ve 2661 d.nm, respectively; PdI values were measured as 0.859 for 100 mg/ml, 0.872 for 50 mg/ml and 1 for the rest. After blender and centrifuge the sample was sonicated for 4 minutes and the mixture was named as triangle. Particle size and PdI of the triangle were measured as 647 d.nm and 0.897. Triangle was centrifuged and the pellet was named square. Particle sizes of the square dilutions were measured as 959 d.nm for 100 mg/ml, 697 d.nm for 50 mg/ml, 901 d.nm for 25 mg/ml, 1023 d.nm for 12.5 mg/ml, 910 d.nm for 6.5 mg/ml. PdI values were measured for the same concentrations as 0.978, 0.981, 1, 0.946, and 0.937, respectively. Square was sonicated for 4 minutes and the end mixture was named circle. Z-average of the circle was measured as 624 d.nm and the PdI was measured as 0.640. Pellet formed after centrifugation of the circle was named star. Particle size of star's different concentrations was measured as 2492 d.nm for 100 mg/ml, 1441 d.nm for 50 mg/ml, 1372 d.nm for 25 mg/ml, 1577 d.nm for 12.5 mg/ml, and 1199 d.nm for 6.5 mg/ml. PdI values were measured as 0.657 for 100 mg/ml, 0.924 mg/ml, and 1 for the rest of the concentrations.

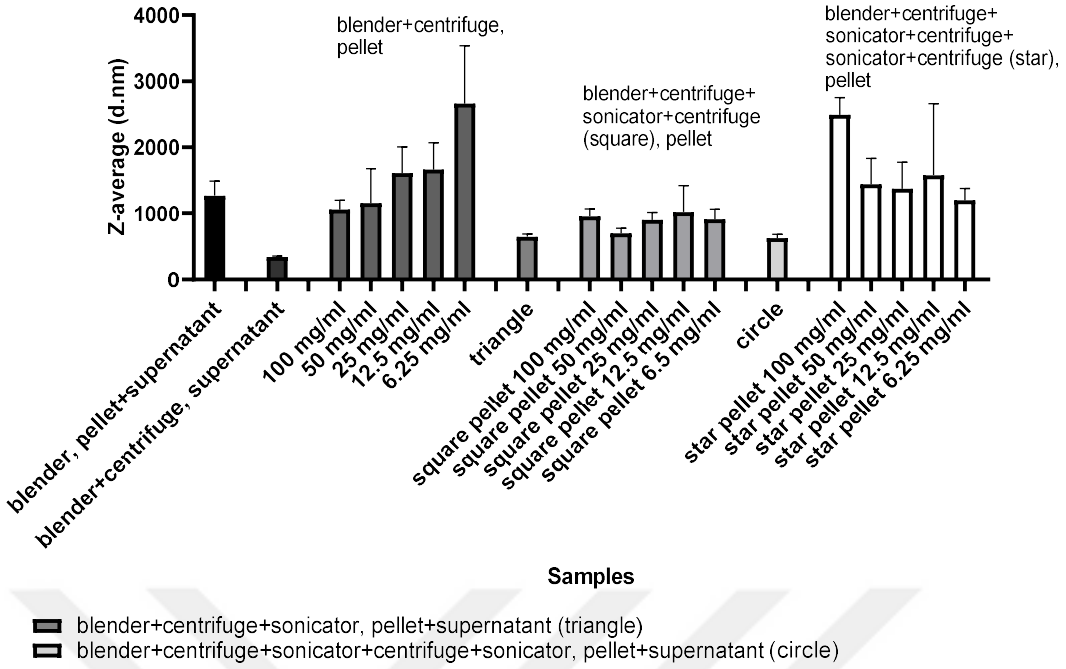

Figure 3.9. Z-average of 1:35 hydrogels shredded with blender and sonicator

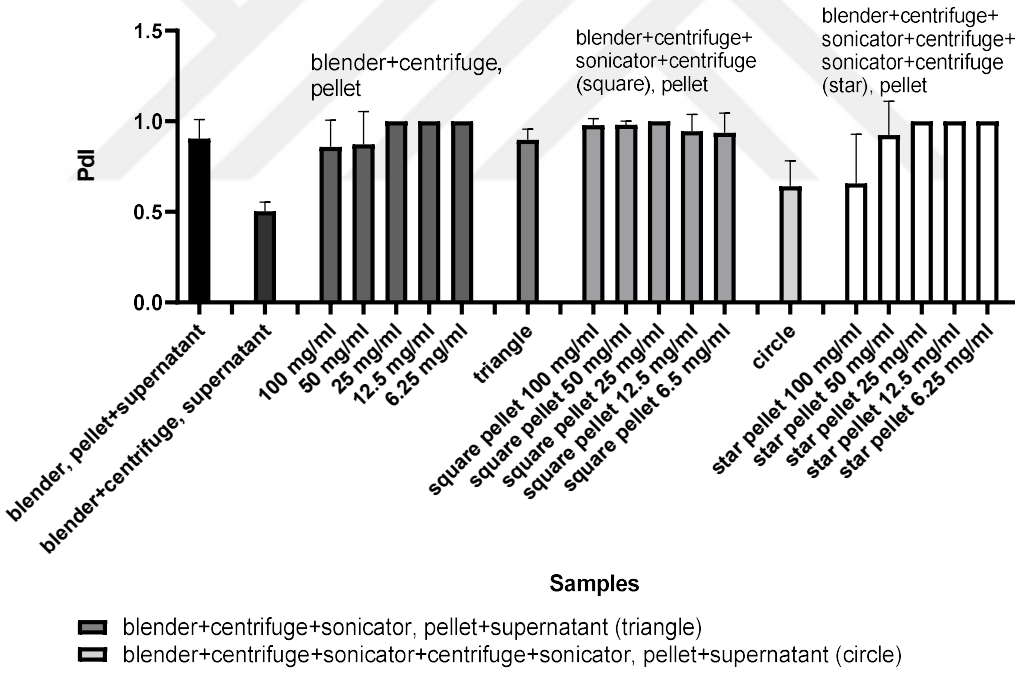

Figure 3.10. PdI of 1:35 hydrogels shredded with blender and sonicator

Close and equal to 1 PdI of the pellets were collected from blender and sonicator applied hydrogels shows that the repeated sonication did not help obtaining a monodisperse hydrogel. Moreover, a stable size decrease was also not observed after sonication. Thus, grinded hydrogels were chosen for further experiments due to ease of the process.

3.6. CBD Release Test

CBD loading was performed to test the CBD release from the hydrogels. EtOH/CBD/distilled water soaked 1:35 ground hydrogels were used in the release test. Release graph of the hydrogels swollen in 1, 2.5, and 12.15 mg/ml CBD was given in Figure 3.11.. Highest release as 0.00211 mg/ml was obtained from the hydrogel swollen in 1 mg/ml CBD. Lowest release was obtained from the hydrogel swollen in 12.15 mg/ml CBD. A rapid initial release (burst release) was not observed.

Release tests performed with the dialysis tube. Dialysis tube was used to prevent the hydrogel and the possible released levan interfering with the release media. During swelling, stuck CBD was observed on the plastic test tubes, especially with the high concentration CBD samples. Therefore, it was thought that the CBD detection in the release medium was lower than expected due to deficient penetration of the CBD.

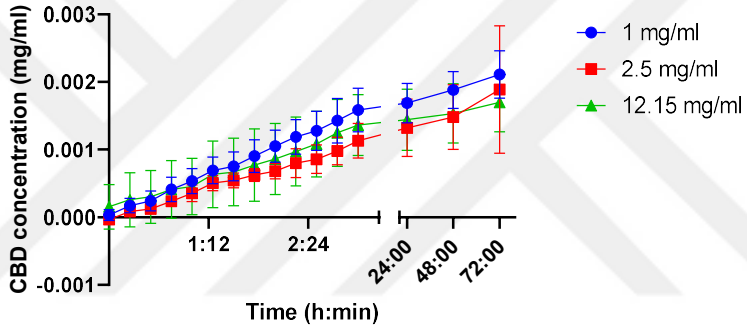

Figure 3.11. Cumulative release of CBD from 1:35 ground hydrogels

3.7. Cell Viability Tests

Extracts were obtained from the hydrogels kept in cell medium for 24, 48, and 72 hours and used for HOB cell viability (Figure 3.12.).

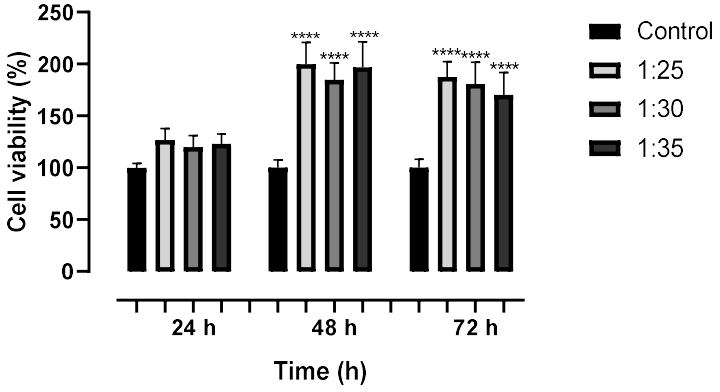

Figure 3.12. Cell viability of HOB cells with hydrogel extracts of 1, 2, and 3 days

Control group was calculated as 100%. Cell viability at 24 hours extract was calculated as 126.79% for 1:25, 119.80% for 1:30, 122.93% for 1:35. For the 48 hours extract, it was calculated as 199.86% for 1:25, 184.51 for 1:30, and 196.81% for 1:35. Cell viability at 72 hours extract was calculated as 187.64% for 1:25, 180.57% for 1:30, and 170.28% for 1:35. A significant difference in cell viability of HOB cells was observed at 48 and 72 hours extracts. Thus, extract of the levan hydrogels was found biocompatible to the HOB cells. Even, it supported cell proliferation. Previously, a good biocompatibility was recorded by our team for hydrolyzed *Halomonas* levan with PCS-201-012 (Human fibroblast cell line) (Erginer et al., 2023).

Biocompatibility of hydrogels were tested after getting swollen with distilled water, cut into one size with a surgical sponge, and dried in a lyophilizer. Cell viability of the hydrogels were tested with CCK-8 kit for 24, 48, and 72 hours. Figure 3.13. shows the cell viability percentages of HOB cells for each day.

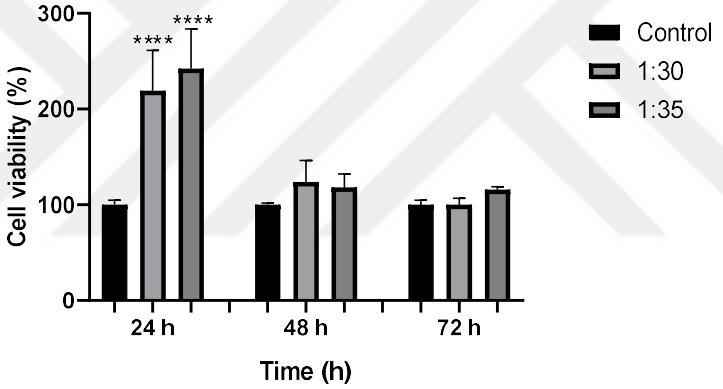

Figure 3.13. Cell viability of HOB cells on the lyophilized hydrogel pieces

All the control groups were calculated as 100%. At the end of 24 hours, cell viability with 1:30 and 1:35 hydrogels were calculated as 219.21% and 242.11%, respectively. Second day, cell viability with 1:30 and 1:35 hydrogels were 123.94% and 117.89%, respectively. After 72 hours of incubation, cell viability with 1:30 and 1:35 hydrogels were calculated as 99.84% and 115.55%, respectively. A significant increasing cell viability difference at 24 hours of incubation of the HOB cells with 1:30 and 1:35 hydrogels was observed. At the end of 72 hours, direct contact of the hydrogels to the HOB cells did not have a negative effect compared to control. First day, due to media uptake into dry hydrogels there was fresh media flow into the hydrogels. The cells that possibly found in the pores of the hydrogel had access to the fresh media. After reaching a relatively stable state of swelling, at day two and three, it was thought

that the observed cell viability decrease could be explained as the nutrient and oxygen deficiency inside the hydrogels. Literature supports that during the cytotoxicity test of porous structures, media components can be absorbed by the biomaterial and this situation may reflect increased cytotoxicity (Podgórski et al., 2022). At least 72 hours of incubation with the porous biomaterial is recommended to be able to observe the cell viability of the cells that adapted to the environment.

Cell viability of HOB cells incubated with lyophilized ground hydrogels for 72 hours was examined (Figure 3.14.). Control group was calculated as 100% and cell viability of HOB cells with 1:25, 1:30, and 1:35 hydrogels was calculated as 85.78%, 109.54%, and 139.88%, respectively. No significant difference was observed at any hydrogel group compared to the control group.

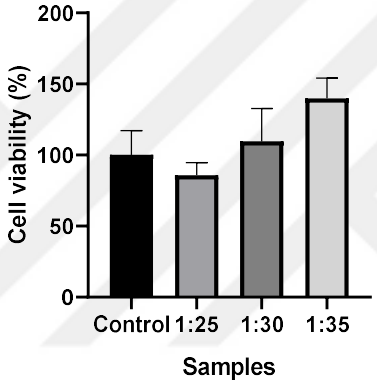

Figure 3.14. Cell viability of HOB cells on the ground lyophilized hydrogels at the end of 72 hours

Ground hydrogels showed higher biocompatibility compared to a piece of the hydrogel at the end of 72 hours. Increasing released hydrogel content (most likely hydrolyzed levan) was expected from ground hydrogels due to increasing surface area. Accordingly, the increasing cell viability of the ground hydrogels compared to the hydrogel pieces can be explained by possible increased extraction.

CBD/EtOH applied HOB cells showed 85.53% cell viability compared to control at 0.004 mg/ml concentration (Figure 3.15.). 72.43% cell viability was observed with 0.008 mg/ml CBD/EtOH. As the concentration continued to increase, cell viability decreased to 10.5%. When the result of the release test was considered, 0.002 mg/ml CBD releasing hydrogels have the potential to be non-toxic to HOB cells.

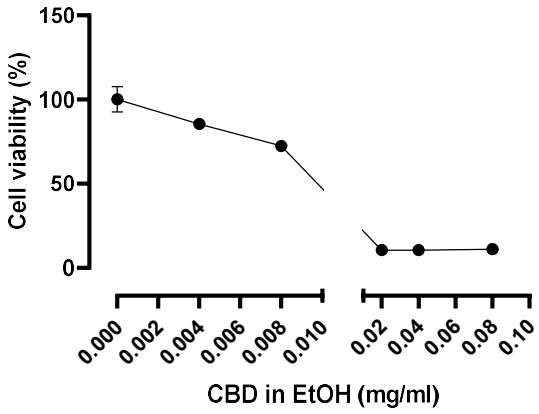

Figure 3.15. Cell viability of HOB cells treated with CBD/EtOH.

CBD/methanol-treated melanoma cells showed decrease in cell number significantly compared to control at the concentrations of 0.2 and 0.04 mg/ml while 0.008 mg/ml treated cells showed close cell counts to the control group (Burch, et al., 2021). In another study, lipopolysaccharide induced RAW264.7 cells were exposed to CBD dissolved in DMSO (Wang et al., 2022). Concentrations less than 0.008 mg/ml were found non-toxic according to these studies. When the HOB cell line compared to these cancer cell lines, it was found more sensitive to CBD.

4. CONCLUSIONS AND RECOMMENDATIONS

MRONJ is a painful disease with open wounds and jawbone loss in later stages. Since it is known that extraction of the tooth or after the treatment of a gum disease together with the usage of certain medicines used for bone protection cause the disease, there is an opportunity to predict and prevent the disease or treat it in the beginning stage (Hasegawa et al., 2017). Levan is known with its biocompatible, anti-inflammatory, and antioxidant, properties which makes it favorable for tissue engineering. CBD is known with its pain killer, and antiinflammatory effects. They have been considered a proper duo for prevention of the disease and keep the area calm and supported in terms of cell proliferation. Thus, *Halomonas* levan hydrogel with CBD as an active reagent was developed to prevent MRONJ disease.

Gel fraction and swelling was examined to understand the characteristics of the *Halomonas* levan/BDDE hydrogels. High gel content, that means a great degree of covalent bonding, was observed in both ground and whole hydrogels. When the hydrogel was shredded, the degree of the covalent bonding decreased. In the conditions of oral cavity (PBS (7.4), at 37°C), the highest swelling degree was observed as 15.95 g/g with the 1:35 levan hydrogel. Therefore 1:35

hydrogels were chosen for shredding and release experiments. Monodispersity could not be obtained by shredding the hydrogels. Further investigations can be conducted to obtain more homogenous hydrogel paste.

Hydrogels loaded with CBD should be directly tested for their cell viability. Either the extract and the hydrogel itself can be tested in further studies. Wound healing and vascularization can be important in terms of preventing the disease that causes cell death. Therefore, these further tests would be effective to understand how the bone cells are reacting to the hydrogels and CBD, besides cell viability. In this thesis, enhanced HOB cell proliferation and proper biocompatibility were shown with the extract, whole, and ground hydrogels.

CBD tends to fail to dissolve in water. Therefore, it was hard to swell a hydrogel, that is supposed to swell in a hydrophilic environment, with CBD. Drug delivery systems such as liposomes, micelles, and nanoparticles can enhance the intake and release of the CBD. However, without using these systems, a drug release was obtained without a burst.

In the scope of this thesis, a CBD loaded ground hydrogel that shows biocompatibility, non-stimuli responsive property, and high gel fraction was developed and gives hope to prevent MRONJ with further *in vivo* and *in vitro* investigations.

REFERENCES

Akgul, B., Gulcan, C., Tornaci, S., Erginer, M., Toksoy Oner, E., Abamor, E. S., ... & Allahverdiyev, A. M. (2024). Manufacturing Radially Aligned PCL Nanofibers Reinforced With Sulfated Levan and Evaluation of its Biological Activity for Healing Tympanic Membrane Perforations. *Macromolecular Bioscience*, 2400291.

Al Maruf, D. A., Ghosh, Y. A., Xin, H., Cheng, K., Mukherjee, P., Crook, J. M., ... & Clark, J. R. (2022). Hydrogel: a potential material for bone tissue engineering repairing the segmental mandibular defect. Polymers, 14(19), 4186.

Alonso, J. M., Andrade del Olmo, J., Perez Gonzalez, R., & Saez-Martinez, V. (2021). Injectable hydrogels: From laboratory to industrialization. *Polymers*, *13*(4), 650.

Alonzo, M., Primo, F. A., Kumar, S. A., Mudloff, J. A., Dominguez, E., Fregoso, G., ... & Joddar, B. (2021). Bone tissue engineering techniques, advances, and scaffolds for treatment of bone defects. Current opinion in biomedical engineering, 17, 100248.

AlRowis, R., Aldawood, A., AlOtaibi, M., Alnasser, E., AlSaif, I., Aljaber, A., & Natto, Z. (2022). Medication-related osteonecrosis of the jaw (MRONJ): a review of pathophysiology, risk factors, preventive measures and treatment strategies. *The Saudi Dental Journal*, *34*(3), 202-210.

Andrade del Olmo, J., Pérez-Álvarez, L., Sáez Martínez, V., Benito Cid, S., Pérez González, R., Vilas-Vilela, J. L., & Alonso, J. M. (2022). Drug delivery from hyaluronic Acid–BDDE injectable hydrogels for antibacterial and anti-inflammatory applications. *Gels*, *8*(4), 223.

Avsar, G., Agirbasli, D., Agirbasli, M. A., Gunduz, O., & Oner, E. T. (2018). Levan based fibrous scaffolds electrospun via co-axial and single-needle techniques for tissue engineering applications. Carbohydrate Polymers, 193, 316-325.

Baines, D. K., Wright, K., & Douglas, T. E. (2024). Preliminary In Vitro Assessment of Whey Protein Isolate Hydrogel with Cannabidiol as a Potential Hydrophobic Oral Drug Delivery System for Colorectal Cancer Therapy. *Polymers*, *16*(23), 3273.

Bashir, S., Hina, M., Iqbal, J., Rajpar, A. H., Mujtaba, M. A., Alghamdi, N. A., ... & Ramesh, S. (2020). Fundamental concepts of hydrogels: Synthesis, properties, and their applications. Polymers, 12(11), 2702.

Battafarano, G., Rossi, M., De Martino, V., Marampon, F., Borro, L., Secinaro, A., & Del Fattore, A. (2021). Strategies for bone regeneration: from graft to tissue engineering. *International journal of molecular sciences*, *22*(3), 1128.

Bhunia, S., Kolishetti, N., Arias, A. Y., Vashist, A., & Nair, M. (2022). Cannabidiol for neurodegenerative disorders: A comprehensive review. *Frontiers in pharmacology*, *13*, 989717.

Boccaccini, A. R., Ma, P. X., & Liverani, L. (Eds.). (2021). *Tissue engineering using ceramics and polymers*. Woodhead Publishing.

Bostan, M. S., Mutlu, E. C., Kazak, H., Keskin, S. S., Oner, E. T., & Eroglu, M. S. (2014). Comprehensive characterization of chitosan/PEO/levan ternary blend films. *Carbohydrate polymers*, *102*, 993-1000.

Breeland, G., Sinkler, M. A., & Menezes, R. G. (2023). Embryology, bone ossification. In *StatPearls [Internet]*. StatPearls Publishing.

Bridgeman, M. B., & Abazia, D. T. (2017). Medicinal cannabis: history, pharmacology, and implications for the acute care setting. *Pharmacy and therapeutics*, *42*(3), 180.

Brierly, G. I., Ren, J., Baldwin, J., Saifzadeh, S., Theodoropoulos, C., Tsurkan, M. V., ... & Bray, L. J. (2019). Investigation of sustained BMP delivery in the prevention of medication-related osteonecrosis of the jaw (MRONJ) in a rat model. *Macromolecular bioscience*, *19*(11), 1900226.

Burch, R., Mortuza, A., Blumenthal, E., & Mustafa, A. (2021). Effects of cannabidiol (CBD) on the inhibition of melanoma cells in vitro. Journal of Immunoassay and Immunochemistry, 42(3), 285-291.

Campora, S., Mohsen, R., Passaro, D., Samir, H., Ashraf, H., Al-Mofty, S. E. D., ... & Ghersi, G. (2021). Functionalized poly (N-isopropylacrylamide)-based microgels in tumor targeting and drug delivery. *Gels*, *7*(4), 203.

Chamkouri, H., & Chamkouri, M. (2021). A review of hydrogels, their properties and applications in medicine. *Am. J. Biomed. Sci. Res*, *11*(6), 485-493.

Chua, K., Khan, I., Malhotra, R., & Zhu, D. (2021). Additive manufacturing and 3D printing of metallic biomaterials. *Engineered Regeneration*, *2*, 288-299.

Cinan, E., Cesur, S., Erginer Haskoylu, M., Gunduz, O., & Toksoy Oner, E. (2021). Resveratrol-Loaded Levan Nanoparticles Produced by Electrohydrodynamic Atomization Technique. *Nanomaterials*, *11*(10), 2582.

Clouse, G., Penman, S., Hadjiargyrou, M., Komatsu, D. E., & Thanos, P. K. (2022). Examining the role of cannabinoids on osteoporosis: a review. *Archives of Osteoporosis*, *17*(1), 146.

Costa, R. R., Neto, A. I., Calgeris, I., Correia, C. R., Pinho, A. C., Fonseca, J., ... & Mano, J. F. (2013). Adhesive nanostructured multilayer films using a bacterial exopolysaccharide for biomedical applications. *Journal of Materials Chemistry B*, *1*(18), 2367-2374.

De Siqueira, E. C., de Souza Rebouças, J., Pinheiro, I. O., & Formiga, F. R. (2020). Levan-based nanostructured systems: An overview. *International Journal of Pharmaceutics*, *580*, 119242.

Dec, P., Modrzejewski, A., & Pawlik, A. (2022). Existing and novel biomaterials for bone tissue engineering. International Journal of Molecular Sciences, 24(1), 529.

Desai, S., Bidanda, B., & Bártolo, P. J. (2021). Emerging trends in the applications of metallic and ceramic biomaterials. *Bio-materials and prototyping applications in medicine*, 1-17.

Dirksen, M., Dargel, C., Meier, L., Brändel, T., & Hellweg, T. (2020). Smart microgels as drug delivery vehicles for the natural drug aescin: Uptake, release and interactions. *Colloid and Polymer Science*, *298*, 505-518.

Erginer, M., Akcay, A., Coskunkan, B., Morova, T., Rende, D., Bucak, S., ... & Oner, E. T. (2016). Sulfated levan from Halomonas smyrnensis as a bioactive, heparin-mimetic glycan for cardiac tissue engineering applications. *Carbohydrate polymers*, *149*, 289-296.

Erginer, M., Gökalsin, B., Tornaci, S., Sesal, C., & Öner, E. T. (2023). Exploring the potential of Halomonas levan and its derivatives as active ingredients in cosmeceutical and skin regenerating formulations. *International Journal of Biological Macromolecules*, *240*, 124418.

Erten Taysi, A., Cevher, E., Sessevmez, M., Olgac, V., Mert Taysi, N., & Atalay, B. (2019). The efficacy of sustained-release chitosan microspheres containing recombinant human parathyroid hormone on MRONJ. *Brazilian Oral Research*, *33*, e086.

Eskandari, Z., Bahadori, F., Yenigun, V. B., Demiray, M., Eroğlu, M. S., Kocyigit, A., & Oner, E. T. (2021). Levan enhanced the NF-κB suppression activity of an oral nano PLGA-curcumin

formulation in breast cancer treatment. *International Journal of Biological Macromolecules*, *189*, 223-231.

Feng, Q., Li, D., Li, Q., Cao, X., & Dong, H. (2022). Microgel assembly: Fabrication, characteristics and application in tissue engineering and regenerative medicine. *Bioactive materials*, *9*, 105-119.

Fleisch, H., Reszka, A., Rodan, G., & Rogers, M. (2002). Bisphosphonates: mechanisms of action. *Principles of bone biology*, 1361-XLIII.

Florencio-Silva, R., Sasso, G. R. D. S., Sasso-Cerri, E., Simões, M. J., & Cerri, P. S. (2015). Biology of bone tissue: structure, function, and factors that influence bone cells. *BioMed research international*, *2015*(1), 421746.

Fraile-Martínez, O., García-Montero, C., Coca, A., Álvarez-Mon, M. A., Monserrat, J., Gómez-Lahoz, A. M., ... & Ortega, M. A. (2021). Applications of polymeric composites in bone tissue engineering and jawbone regeneration. *Polymers*, *13*(19), 3429.

Gan, L., Jiang, G., Yang, Y., Zheng, B., Zhang, S., Li, X., ... & Peng, B. (2022). Development and characterization of levan/pullulan/chitosan edible films enriched with ε-polylysine for active food packaging. *Food Chemistry*, *388*, 132989.

Ghandforoushan, P., Alehosseini, M., Golafshan, N., Castilho, M., Dolatshahi-Pirouz, A., Hanaee, J., ... & Orive, G. (2023). Injectable hydrogels for cartilage and bone tissue regeneration: A review. *International Journal of Biological Macromolecules*, *246*, 125674.

Ghasemi, S., Davoodi, P., Boojar, F. M. A., & Dashti, M. (2022). Efficacy of utilizing cannabidiol in reduction of inflammation and autoimmunity manifestation. *Open Access Research Journal of Biology and Pharmacy*, *4*, 040-047.

Gheorghita, R. E., Lupaescu, A. V., Gâtlan, A. M., Dabija, D., Lobiuc, A., Iatcu, O. C., ... & Dabija, A. (2024). Biopolymers-Based Macrogels with Applications in the Food Industry: Capsules with Berry Juice for Functional Food Products. *Gels*, *10*(1), 71.

Grimaudo, M. A., Concheiro, A., & Alvarez-Lorenzo, C. (2019). Nanogels for regenerative medicine. *Journal of Controlled Release*, *313*, 148-160.

Guo, H., Wang, H., Gao, M., Deng, H., Zhang, Y., Gong, J., & Zhang, W. (2024). Harnessing the CD44-targeted delivery of self-assembled hyaluronan nanogel to reverse the antagonism

between Cisplatin and Gefitinib in NSCLC cancer therapy. *Carbohydrate Polymers*, *344*, 122521.

Guo, J., Yao, H., Li, X., Chang, L., Wang, Z., Zhu, W., ... & Xu, J. (2023). Advanced Hydrogel systems for mandibular reconstruction. *Bioactive materials*, *21*, 175-193.

Halligan, E., Tie, B. S. H., Colbert, D. M., Alsaadi, M., Zhuo, S., Keane, G., & Geever, L. M. (2023). Synthesis and characterisation of hydrogels based on poly (N-vinylcaprolactam) with diethylene glycol diacrylate. Gels, 9(6), 439.

Hasegawa, T., Kawakita, A., Ueda, N., Funahara, R., Tachibana, A., Kobayashi, M., ... & Japanese Study Group of Cooperative Dentistry with Medicine (JCDM). (2017). A multicenter retrospective study of the risk factors associated with medication-related osteonecrosis of the jaw after tooth extraction in patients receiving oral bisphosphonate therapy: can primary wound closure and a drug holiday really prevent MRONJ?. *Osteoporosis International*, *28*, 2465-2473.

Hasnain, M. S., Ahmad, S. A., Chaudhary, N., Hoda, M. N., & Nayak, A. K. (2019). Biodegradable polymer matrix nanocomposites for bone tissue engineering. In Applications of nanocomposite materials in orthopedics (pp. 1-37). Woodhead Publishing.

Heider, C. G., Itenberg, S. A., Rao, J., Ma, H., & Wu, X. (2022). Mechanisms of cannabidiol (CBD) in cancer treatment: A review. *Biology*, *11*(6), 817.

Hernandez-Gil, I. F. T., Gracia, M. A., del Canto Pingarrón, M., & Jerez, L. B. (2006). Physiological bases of bone regeneration I. Histology and physiology of bone tissue. *Med Oral*, *11*(1), 47-51.

Hesse, B., Langer, M., Varga, P., Pacureanu, A., Dong, P., Schrof, S., ... & Peyrin, F. (2014). Alterations of mass density and 3D osteocyte lacunar properties in bisphosphonate-related osteonecrotic human jaw bone, a synchrotron μCT study. PloS one, 9(2), e88481.

Ho, T. C., Chang, C. C., Chan, H. P., Chung, T. W., Shu, C. W., Chuang, K. P., ... & Tyan, Y. C. (2022). Hydrogels: properties and applications in biomedicine. Molecules, 27(9), 2902.

Iezzi, G., Mangano, C., Barone, A., Tirone, F., Baggi, L., Tromba, G., ... & Giuliani, A. (2020). Jawbone remodeling: a conceptual study based on Synchrotron High-resolution Tomography. Scientific reports, 10(1), 3777.

Ji, W., Wu, Q., Han, X., Zhang, W., Wei, W., Chen, L., ... & Huang, W. (2020). Photosensitive hydrogels: From structure, mechanisms, design to bioapplications. *Science China Life Sciences*, *63*, 1813-1828.

Jiang, A., Zhang, Z., Qiu, X., & Guo, Q. (2024). Medication-related osteonecrosis of the jaw (MRONJ): a review of pathogenesis hypothesis and therapy strategies. *Archives of Toxicology*, *98*(3), 689-708.

Jimi, E., Hirata, S., Osawa, K., Terashita, M., Kitamura, C., & Fukushima, H. (2012). The current and future therapies of bone regeneration to repair bone defects. International journal of dentistry, 2012(1), 148261.

Kalirajan, C., Dukle, A., Nathanael, A. J., Oh, T. H., & Manivasagam, G. (2021). A critical review on polymeric biomaterials for biomedical applications. *Polymers*, *13*(17), 3015.

Kim, J. O., Park, J. K., Kim, J. H., Jin, S. G., Yong, C. S., Li, D. X., ... & Choi, H. G. (2008). Development of polyvinyl alcohol–sodium alginate gel-matrix-based wound dressing system containing nitrofurazone. *International journal of pharmaceutics*, *359*(1-2), 79-86.

Kırtel, O., & Combie, J. (2022). Levan. In *Polysaccharides of Microbial Origin: Biomedical Applications* (pp. 23-42). Cham: Springer International Publishing.

Kırtel, O., Lescrinier, E., Van den Ende, W., & Öner, E. T. (2019). Discovery of fructans in Archaea. Carbohydrate polymers, 220, 149-156.

Kirtel, Onur et al. 2018. "Levansucrase from Halomonas Smyrnensis AAD6T: First Halophilic GH-J Clan Enzyme Recombinantly Expressed, Purified, and Characterized." Applied Microbiology and Biotechnology 102(21): 9207–20.

Klein, M., & Poverenov, E. (2020). Natural biopolymer-based hydrogels for use in food and agriculture. *Journal of the Science of Food and Agriculture*, *100*(6), 2337-2347.

Klein, M., de Quadros De Bortolli, J., Guimarães, F. S., Salum, F. G., Cherubini, K., & de Figueiredo, M. A. Z. (2018). Effects of cannabidiol, a Cannabis sativa constituent, on oral wound healing process in rats: Clinical and histological evaluation. *Phytotherapy Research*, *32*(11), 2275-2281.

Kołodziejska, B., Kaflak, A., & Kolmas, J. (2020). Biologically inspired collagen/apatite composite biomaterials for potential use in bone tissue regeneration—A review. *Materials*, *13*(7), 1748.

Kongkadee, K., Wisuitiprot, W., Ingkaninan, K., & Waranuch, N. (2022). Anti-inflammation and gingival wound healing activities of Cannabis sativa L. subsp. sativa (hemp) extract and cannabidiol: An in vitro study. *Archives of Oral Biology*, *140*, 105464.

Koons, G. L., Diba, M., & Mikos, A. G. (2020). Materials design for bone-tissue engineering. Nature Reviews Materials, 5(8), 584-603.

Kuźnik, A., Październiorok-Holewa, A., Jewula, P., & Kuźnik, N. (2020). Bisphosphonates—much more than only drugs for bone diseases. *European journal of pharmacology*, *866*, 172773.

Lima, C. S. D., Balogh, T. S., Varca, J. P., Varca, G. H., Lugão, A. B., A. Camacho-Cruz, L., ... & Kadlubowski, S. S. (2020). An updated review of macro, micro, and nanostructured hydrogels for biomedical and pharmaceutical applications. *Pharmaceutics*, *12*(10), 970.

Lu, H. D., Charati, M. B., Kim, I. L., & Burdick, J. A. (2012). Injectable shear-thinning hydrogels engineered with a self-assembling Dock-and-Lock mechanism. *Biomaterials*, *33*(7), 2145-2153.

Lu, Y., Zhao, M., Peng, Y., He, S., Zhu, X., Hu, C., ... & Shen, X. (2022). A physicochemical double-cross-linked gelatin hydrogel with enhanced antibacterial and anti-inflammatory capabilities for improving wound healing. *Journal of Nanobiotechnology*, *20*(1), 426.

Morakul, B., Junyaprasert, V. B., Sakchaisri, K., & Teeranachaideekul, V. (2023). Cannabidiol-loaded nanostructured lipid carriers (NLCs) for dermal delivery: enhancement of photostability, cell viability, and anti-inflammatory activity. *Pharmaceutics*, *15*(2), 537.

Newsom, J. P., Payne, K. A., & Krebs, M. D. (2019). Microgels: Modular, tunable constructs for tissue regeneration. *Acta biomaterialia*, *88*, 32-41.

Ning, H., Wu, X., Wu, Q., Yu, W., Wang, H., Zheng, S., ... & Su, J. (2019). Microfiber-reinforced composite hydrogels loaded with rat adipose-derived stem cells and BMP-2 for the treatment of medication-related osteonecrosis of the jaw in a rat model. *ACS Biomaterials Science & Engineering*, *5*(5), 2430-2443.

Omi, M., & Mishina, Y. (2021). Role of osteoclasts in oral homeostasis and jawbone diseases. Oral science international, 18(1), 14-27.

On, S. W., Cho, S. W., Byun, S. H., & Yang, B. E. (2021). Various therapeutic methods for the treatment of medication-related osteonecrosis of the jaw (MRONJ) and their limitations: A

narrative review on new molecular and cellular therapeutic approaches. *Antioxidants*, *10*(5), 680.

Overstreet, D. J., Dutta, D., Stabenfeldt, S. E., & Vernon, B. L. (2012). Injectable hydrogels. *Journal of Polymer Science Part B: Polymer Physics*, *50*(13), 881-903.

Park, J. B., & Lakes, R. S. (2007). Composites as biomaterials. *Biomaterials*, 207-224.

Park, J., & Lakes, R. S. (2007). *Biomaterials: an introduction*. Springer Science & Business Media.

Patel, P., & Thareja, P. (2022). Hydrogels differentiated by length scales: A review of biopolymer-based hydrogel preparation methods, characterization techniques, and targeted applications. *European Polymer Journal*, *163*, 110935.

Peng, J., Fan, M., An, C., Ni, F., Huang, W., & Luo, J. (2022). A narrative review of molecular mechanism and therapeutic effect of cannabidiol (CBD). *Basic & clinical pharmacology & toxicology*, *130*(4), 439-456.

Pisanti, S., Malfitano, A. M., Ciaglia, E., Lamberti, A., Ranieri, R., Cuomo, G., ... & Bifulco, M. (2017). Cannabidiol: State of the art and new challenges for therapeutic applications. *Pharmacology & therapeutics*, *175*, 133-150.

Podgórski, R., Wojasiński, M., & Ciach, T. (2022). Nanofibrous materials affect the reaction of cytotoxicity assays. Scientific reports, 12(1), 9047.

Poli, A., Kazak, H., Gürleyendağ, B., Tommonaro, G., Pieretti, G., Öner, E. T., & Nicolaus, B. (2009). High level synthesis of levan by a novel Halomonas species growing on defined media. *Carbohydrate polymers*, *78*(4), 651-657.

Poli, A., Nicolaus, B., Denizci, A. A., Yavuzturk, B., & Kazan, D. (2013). Halomonas smyrnensis sp. nov., a moderately halophilic, exopolysaccharide-producing bacterium. *International journal of systematic and evolutionary microbiology*, *63*(Pt_1), 10-18.

Punj, S., Singh, J., & Singh, K. J. C. I. (2021). Ceramic biomaterials: Properties, state of the art and future prospectives. *Ceramics International*, *47*(20), 28059-28074.

Rafael, D., Melendres, M. M. R., Andrade, F., Montero, S., Martinez-Trucharte, F., Vilar-Hernandez, M., ... & Abasolo, I. (2021). Thermo-responsive hydrogels for cancer local therapy: Challenges and state-of-art. *International journal of pharmaceutics*, *606*, 120954.

Rajabi, M., McConnell, M., Cabral, J., & Ali, M. A. (2021). Chitosan hydrogels in 3D printing for biomedical applications. Carbohydrate Polymers, 260, 117768.

Raman, R., Hua, T., Gwynne, D., Collins, J., Tamang, S., Zhou, J., ... & Traverso, G. (2020). Light-degradable hydrogels as dynamic triggers for gastrointestinal applications. *Science advances*, *6*(3), eaay0065.

Rizzo, F., & Kehr, N. S. (2021). Recent advances in injectable hydrogels for controlled and local drug delivery. *Advanced healthcare materials*, *10*(1), 2001341.

Samadian, H., Maleki, H., Allahyari, Z., & Jaymand, M. (2020). Natural polymers-based light-induced hydrogels: Promising biomaterials for biomedical applications. *Coordination Chemistry Reviews*, *420*, 213432.

Sarilmiser, H. K., & Oner, E. T. (2014). Investigation of anti-cancer activity of linear and aldehyde-activated levan from Halomonas smyrnensis AAD6T. *Biochemical engineering journal*, *92*, 28-34.

Selvi, S. S., Hasköylü, M. E., Genç, S., & Toksoy Öner, E. (2021). Synthesis and characterization of levan hydrogels and their use for resveratrol release. *Journal of Bioactive and Compatible Polymers*, *36*(6), 464-480.

Sezer, A. D., Kazak, H., Öner, E. T., & Akbuğa, J. (2011). Levan-based nanocarrier system for peptide and protein drug delivery: Optimization and influence of experimental parameters on the nanoparticle characteristics. *Carbohydrate Polymers*, *84*(1), 358-363.

Shafiq, M., Rafique, M., Cui, Y., Pan, L., Do, C. W., & Ho, E. A. (2023). An insight on ophthalmic drug delivery systems: focus on polymeric biomaterials-based carriers. *Journal of Controlled Release*, *362*, 446-467.

Sharma, D., Hamlet, S., Vaquette, C., Petcu, E. B., Ramamurthy, P., & Ivanovski, S. (2021). Local delivery of hydrogel encapsulated vascular endothelial growth factor for the prevention of medication-related osteonecrosis of the jaw. *Scientific Reports*, *11*(1), 23371.

Sima, F., Axente, E., Sima, L. E., Tuyel, U., Eroglu, M. S., Serban, N., ... & Mihailescu, I. N. (2012). Combinatorial matrix-assisted pulsed laser evaporation: single-step synthesis of biopolymer compositional gradient thin film assemblies. *Applied Physics Letters*, *101*(23).

Sivasankarapillai, V. S., Das, S. S., Sabir, F., Sundaramahalingam, M. A., Colmenares, J. C., Prasannakumar, S., ... & Kyzas, G. Z. (2021). Progress in natural polymer engineered biomaterials for transdermal drug delivery systems. *Materials Today Chemistry*, *19*, 100382.

Sosnik, A., Shabo, R. B., & Halamish, H. M. (2021). Cannabidiol-loaded mixed polymeric micelles of chitosan/poly (vinyl alcohol) and poly (methyl methacrylate) for trans-corneal delivery. *Pharmaceutics*, *13*(12), 2142.

Srikanth, R., Reddy, C. H. S., Siddartha, G., Ramaiah, M. J., & Uppuluri, K. B. (2015). Review on production, characterization and applications of microbial levan. *Carbohydrate polymers*, *120*, 102-114.

Stojkov, G., Niyazov, Z., Picchioni, F., & Bose, R. K. (2021). Relationship between structure and rheology of hydrogels for various applications. *Gels*, *7*(4), 255.

Sun, A., He, X., Ji, X., Hu, D., Pan, M., Zhang, L., & Qian, Z. (2021). Current research progress of photopolymerized hydrogels in tissue engineering. *Chinese Chemical Letters*, *32*(7), 2117-2126.

Suzuki, S., Venkataiah, V. S., Yahata, Y., Kitagawa, A., Inagaki, M., Njuguna, M. M., ... & Saito, M. (2022). Correction of large jawbone defect in the mouse using immature osteoblast–like cells and a 3D polylactic acid scaffold. PNAS nexus, 1(4), pgac151.

Toksoy Oner, E., Hernández, L., & Combie, J. (2016). Review of Levan polysaccharide: From a century of past experiences to future prospects. *Biotechnology advances*, *34*(5), 827-844.

Tomulescu, C., Stoica, R., Sevcenco, C., Casarica, A., Moscovici, M., & Vamanu, A. (2016). Levan-a mini review. *Scientific Bulletin Series F. Biotechnologies*, *20*.

Vaiani, L., Boccaccio, A., Uva, A. E., Palumbo, G., Piccininni, A., Guglielmi, P., ... & Ballini, A. (2023). Ceramic materials for biomedical applications: an overview on properties and fabrication processes. *Journal of Functional Biomaterials*, *14*(3), 146.

Venkatesan, J., & Kim, S. K. (2010). Chitosan composites for bone tissue engineering—an overview. *Marine drugs*, *8*(8), 2252-2266.

Wang, J., Viola, M., Migliorini, C., Paoletti, L., Arpicco, S., Di Meo, C., & Matricardi, P. (2023). Polysaccharide-Based Nanogels to Overcome Mucus, Skin, Cornea, and Blood-Brain Barriers: A Review. *Pharmaceutics*, *15*(10), 2508.

Wang, Y., Wang, X., Yang, Y., Quan, Q., Huo, T., Yang, S., ... & An, Q. (2022). Comparison of the in vitro Anti-Inflammatory Effect of Cannabidiol to Dexamethasone. Clinical, Cosmetic and Investigational Dermatology, 1959-1967.

Wilde, F., Heufelder, M., Winter, K., Hendricks, J., Frerich, B., Schramm, A., & Hemprich, A. (2011). The role of surgical therapy in the management of intravenous bisphosphonates-related osteonecrosis of the jaw. *Oral Surgery, Oral Medicine, Oral Pathology, Oral Radiology, and Endodontology*, *111*(2), 153-163.

Wu, R. S., Lin, J., Xing, Y. M., Dai, Z. L., Wang, L. W., & Zhang, X. P. (2019). pH-sensitive black phosphorous–incorporated hydrogel as novel implant for cancer treatment. *Journal of Pharmaceutical Sciences*, *108*(8), 2542-2551.

Xu, C., Liu, Z., Chen, X., Gao, Y., Wang, W., Zhuang, X., ... & Dong, X. (2024). Bone tissue engineering scaffold materials: Fundamentals, advances, and challenges. *Chinese Chemical Letters*, *35*(2), 109197.

Xu, W., Lu, F., Chen, S., Lin, X., Zhou, S., & Wu, W. (2017). Synthesis of polymer macrogels with rapid and significant response to glucose concentration changes. *RSC advances*, *7*(88), 55945-55956.

Xue, X., Hu, Y., Wang, S., Chen, X., Jiang, Y., & Su, J. (2022). Fabrication of physical and chemical crosslinked hydrogels for bone tissue engineering. *Bioactive materials*, *12*, 327-339.

Yang, C., Blum, N. T., Lin, J., Qu, J., & Huang, P. (2020). Biomaterial scaffold-based local drug delivery systems for cancer immunotherapy. *Science Bulletin*, *65*(17), 1489-1504.

Yang, J., Gong, C., Shi, F. K., & Xie, X. M. (2012). High strength of physical hydrogels based on poly (acrylic acid)-g-poly (ethylene glycol) methyl ether: role of chain architecture on hydrogel properties. The Journal of Physical Chemistry B, 116(39), 12038-12047.

Yu, Y., Cheng, Y., Tong, J., Zhang, L., Wei, Y., & Tian, M. (2021). Recent advances in thermo-sensitive hydrogels for drug delivery. *Journal of Materials Chemistry B*, *9*(13), 2979-2992.

Zhang, M., & Zhao, X. (2020). Alginate hydrogel dressings for advanced wound management. *International Journal of Biological Macromolecules*, *162*, 1414-1428.

Zhuo, S., Zhang, F., Yu, J., Zhang, X., Yang, G., & Liu, X. (2020). pH-sensitive biomaterials for drug delivery. *Molecules*, *25*(23), 5649.

AUTOBIOGRAPHY

Name Surname Ece Özyağcı

Education

Master's degree **2022-Still** Institute of Pure and Applied Sciences - Department of Bioengineering - Marmara University

Bachelor's degree **2016-2021** Faculty of Engineering, Department of Genetics and Bioengineering - Yeditepe University

Exchange Program

2019 Faculty 4: Energy-, Process-, and Bio-Engineering - Stuttgart University

Projects

M-ERA.NET "Inject-Bio - Bioactive injectable hydrogels for soft tissue regeneration after reconstructive maxillofacial surgeries" supported by TUBITAK with the project no: 119N756

Presentations

Ece Özyağcı, Selay Tornacı, Ebru Toksoy Öner, "Biyomedikal Uygulamaları için CBD Yüklü Levan Hidrojellerin Sentezi ve Karakterizasyonu" VIII. Ulusal Biyomühendislik Kongresi "Biyomühendislik Uygulamaları", 16-18 May 2024, Manisa, Turkey (Poster presentation)

Selay Tornacı, M. Yusuf Kandur, Ece Özyağcı, Ebru Toksoy Öner, "Levan Based Hydrogels for Biomedical Applications" IX. International Fructan Symposium 10-13 October 2022, Istanbul, Turkey (Poster Presentation)